A REPORT ON THE GRAVITATIONAL REDSHIFT TEST FOR NON-METRIC THEORIES OF GRAVITATION

FINAL REPORT

GRANT NSG-8059

Prepared for

NATIONAL AERONAUTICS and SPACE ADMINISTRATION

GEORGE C. MARSHALL SPACE FLIGHT CENTER

MARSHALL SPACE FLIGHT CENTER, ALABAMA 35812

August, 1980

Smithsonian Institution
Astrophysical Observatory
Cambridge, Massachusetts 02138

(NASA-CR-163496) A REPORT ON THE GRAVITATIONAL REDSHIFT TEST FOR NON-METRIC THEORIES OF GRAVITATION Final Report, 1 Feb. - 31 Aug. 1980 (Smithsonian Astrophysical Observatory) 55 p

N80-30978

G3/46

Unclas
28509

A REPORT ON THE GRAVITATIONAL REDSHIFT TEST FOR NON-METRIC THEORIES OF GRAVITATION

FINAL REPORT

GRANT NSG-8059

Prepared for

NATIONAL AERONAUTICS and SPACE ADMINISTRATION

GEORGE C. MARSHALL SPACE FLIGHT CENTER

MARSHALL SPACE FLIGHT CENTER, ALABAMA 35812

August, 1980

Smithsonian Institution
Astrophysical Observatory
Cambridge, Massachusetts 02138

The Smithsonian Astrophysical Observatory
and the Harvard College Obseravtory
are members of the
Center for Astrophysics

ABSTRACT

An experiment to test whether gravitation is described by metric or non-metric theories was carried out by B.F. Farrell, E. M. Mattison, and R.F.C. Vessot of the Smithsonian Astrophysical Observatory and J. Turneaure and C. Will of Stanford University. The frequencies of two atomic hydrogen masers and of three superconducting-cavity stabilized oscillators (SCSOs) were compared as the ensemble of oscillators was moved in the sun's gravitational field by the rotation and orbital motion of the earth. Metric gravitation theories predict that the gravitational redshifts of the two types of oscillators are identical, and that there should be no relative frequency shift between the oscillators; non-metric theories, in contrast, predict a frequency shift between masers and SCSOs that is proportional to the change in solar gravitational potential experienced by the oscillators. The results of the experiment show that

$$\frac{\Delta f/f}{\Delta\phi/c^2} < 2.0\times10^{-2}$$

where $\Delta f/f$ is the relative frequency shift of masers and SCSOs, expressed as a fraction of their frequencies, $\Delta\phi$ is the change in gravitational potential, and c is the speed of light; the limit represents the upper bound of the 95% confidence interval. The results are thus consistent with metric theories of gravitation at a level of 2%.

1. INTRODUCTION:

The development in recent years of extremely high stability frequency sources has given the physicist new tools for testing theories of relativity and gravitation. In the experiment described here, the frequencies of high stability oscillators were compared over periods of several weeks in order to test basic assumptions of relativity theory and to measure the characteristics of the oscillators themselves. The experiment resulted from a conjecture that if gravitation were described by a non-metric theory, clocks based upon different physical principles would run at different rates when the strength of the gravitational field they were exposed to was changed. [1] In this experiment we measured the relative frequencies of two hydrogen masers and three superconducting-cavity stabilized oscillators as the oscillators moved in the gravitational field of the sun as a result of the rotation and revolution of the earth.

The output frequency of the hydrogen maser is based upon the hyperfine splitting of ground state atomic hydrogen. The construction and characteristics of the masers are described in detail in the literature.[2,3] Briefly, hydrogen atoms in the upper hyperfine level ($F = 1$, $m_F = 0$) enter a Teflon-lined quartz sphere contained in an evacuated microwave cavity resonant at the hyperfine frequency (1.42 GHz) and are stimulated to radiate to the lower hyperfine level ($F = 0$, $m_F = 0$) by the microwave field in the cavity. The output frequency is shifted from the hyperfine frequency by interactions of the atoms with the Teflon wall surface, with an imposed axial magnetic field, and with each other, and by variations in the cavity resonance frequency that can be caused by changes in temperature, barometric pressure, mechanical stress, and other sources.

The SCSO consists of an electronic self oscillator whose frequency-determining element is a high-Q superconducting cavity maintained at the temperature of liquid helium. The cavity's dimensions, and thus its resonance frequency (approximately 8 GHz), can be affected by such external effects as temperature and mechanical stress, including stress changes due to variations in the strength of the local gravity field and in the cavity's angle of tilt relative to the vertical.

Section 2 of this report describes the theory underlying the experiment. The experimental procedures and methods of data collection are described in Section 3, and the data analysis is described in Section 4. The conclusions of the experiment are discussed in Section 5.

2. THEORY

This experiment, which tests whether gravitation is described by a metric or a non-metric theory, is based upon the following conjecture: "Every non-metric theory of gravity predicts a gravitational redshift that depends on the nature of the clock whose redshift is being measured."[1] Quantitative predictions are obtained from the Lightman-Lee formalism,[4] which is applicable to certain classes of gravitational theories and which describes the behavior of electromagnetic fields and charged particles in the presence of an external, static, spherically symmetric gravitational potential $U_0 = \frac{GM}{rc^2}$. Here G is the gravitational constant, M the mass of the external body, and r is the distance between the body and the observation point. The potential U_0 is normalized to the square of the speed of light, c. In the limit of a weak gravitational field ($U_0 << 1$) the functions describing the particles and the electromagnetic fields can be expanded in terms of dimensionless parameters Γ_0, $\Gamma_1, \ldots$, T_1, $T_2, \ldots$, whose values depend on the particular gravitational theory being used.

Every metric theory has $\Gamma_i = T_i = 0$ for all i; every non-metric theory has at least one of the Γ's or T's non-zero.

We imagine an experiment in which the frequency of a clock is measured as it moves from one point to another in a gravitational field, with a gravitational potential difference ΔU between observation points. The predicted redshift for a hydrogen maser clock is [1]

$$\left(\frac{\Delta f}{f}\right)_{maser} = (1-4\,\Gamma_o + T_1)\,\Delta U = (1 + \alpha_m)\,\Delta U \qquad (1)$$

For a clock whose frequency is determined by the dimensions of a microwave cavity, such as an SCSO, the redshift prediction is

$$\left(\frac{\Delta f}{f}\right)_{SCSO} = \left(1 - \Gamma_o - \frac{1}{2}\,T_1\right)\Delta U = (1 + \alpha_s)\,\Delta U \qquad (2)$$

If a maser and an SCSO together experience the potential change ΔU, their relative frequency difference will change by :

$$\left(\frac{\Delta f}{f}\right)_M - \left(\frac{\Delta f}{f}\right)_S = \frac{3}{2}\,(T_1 - 2\,\Gamma_o)\,\Delta U = (\alpha_m - \alpha_s)\,\Delta U \equiv \alpha_{ms}\,\Delta U \qquad (3)$$

All metric theories ($T_1 = \Gamma_o = o$) predict that the clocks will not change frequency with respect to one another, that is, $\alpha_{ms} = 0$. In this experiment we attempt to place a bound on the magnitude of α_{ms}.

The largest time-dependent component of gravitational potential seen by the clocks is the variation resulting from the motion of the laboratory in the sun's gravitational field as the earth rotates on its axis and travels in its orbit. The experiment was carried out in Palo Alto, California in late March and early April, 1978. At that time of year the orbital phase of the earth was approximately 90^o with respect to perihelion, and the earth-sun separation was changing at its most rapid rate. Thus the potential has a component changing with a diurnal

period and a component varying nearly linearly with time. The expression for the time-varying part, U, of the potential at the position of Palo Alto is:

$$U(t) = 2.84 \times 10^{-12} (t-t_\star) [1 - 4.9 \times 10^{-5} (t-t_\star)^2] - 3.2 \times 10^{-13} \cos[2\pi (t-t_\star)] \quad (4)$$

Here t is measured in solar days and $t_\star$ = April 4.5 (that is, noon on April 4). The term $(t-t_\star)^2$ in square brackets results from the fact that the radial motion in orbit is described by a sine function with a period of one year; for intervals of the order of tens of days, as in this experiment, the departure from a linear function of time may be ignored. The expression for the lowest-order terms of the time varying gravitational potential, then, is

$$U(t) = 2.84 \times 10^{-12} (t-t_\star) - 3.2 \times 10^{-13} \cos[2\pi (t-t_\star)] \quad (5)$$

3. DESCRIPTION OF EQUIPMENT AND DATA ACQUISITION

3.1. Laboratory Setup

The experiment was performed at Stanford University, Palo Alto, California. Three SCSO's built at the Stanford High Energy Physics Laboratory were contained in a single liquid-helium dewar in a temperature-controlled, isolated inner room within a laboratory area. The dewar's liquid nitrogen shield was cooled by a recirculating refrigerator using helium gas as the transfer medium. This eliminated the need for refilling the dewar during the experiment. The dewar was equipped with a servo-controlled anti-tilt device to reduce the effect of floor tilt on the SCSOs' frequencies. Two model VLG-10 masers, built by the Smithsonian Astrophysical Observatory (SAO), were placed in the outer room of the laboratory. Because the temperature of this room was strongly affected by outside weather conditions, a window air-conditioner with an on/off control was installed. To moderate the temperature variations caused by the cycling of the air-conditioner, the masers were placed in large wooden enclosures equipped with temperature controlled exhaust fans that helped keep the air surrounding the masers at a constant temperature.

3.2 Frequency Comparison and Data Acquisition

The frequencies of the oscillators were compared using the system shown schematically in Figure 1. (The SCSOs are referred to as S1, S2, and S3, and the masers as P5 and P6. Subscripts indicating frequency differences use numerals only: 1, 2, 3, for SCSOs and 5, 6 for masers.) A 5 MHz voltage-controlled crystal oscillator (VCXO) was phase-locked to the output of S1, and its output was multiplied and mixed with the

signals from the four other oscillators, producing beat signals whose periods were measured by counters. The difference frequencies of S1-S2 and S1-S3 were set by means of frequency synthesizers to approximately 5 Hz, while the S1-P5 and S1-P6 beat frequencies were set to approximately 1.2 Hz. The intervals over which the beat periods were averaged are given in Table I.

TABLE I - AVERAGING INTERVALS FOR DIFFERENCE FREQUENCY MEASUREMENTS

Oscillators	Number of Beat Periods Averaged	Approximate Beat Frequency (Hz)	Approximate Averaging Interval (Sec.)
S1-S2	1500	5	300
S1-S3	1500	5	300
S1-P5	100	1.2	83
S1-P6	300	1.2	250

The counters used to measure the average periods between S1 and S2, S1 and S3, and S1 and P6 were zero-deadtime units that did not introduce a time lapse between adjacent samples. The S1-P5 counter had a one-period deadtime and thus introduced a 1 per-cent time lapse between 100-period averaging intervals. Each period measurement was recorded along with the date and the time at the end of the measurement.

An additional frequency measurement system was operated simultaneously with the one described above. The periods of the beat signals S1-P5 and S1-P6 were measured by counters that measured the elapsed period for 100 cycles, with a one-period deadtime between measurements. These data were recorded on magnetic tape by HP9825 calculators. Before and after the experimental runs, measurements over 1-, 10- and 100- period averaging intervals were made and recorded. In addition, before and after the runs the maser frequencies were compared directly by a method similar to that shown in Fig. 1,

in which a 5 MHz VCXO was phase-locked to the output of one of the masers. These pre-and post-run comparisons gave quick checks of the oscillators' stabilites and verified their proper operation.

Measurements of ambient conditions were recorded at forty-minute intervals together with the date and time of each measurement. The types of ambient data measured are given in Table II.

TABLE II - AMBIENT CONDITIONS MONITORED DURING EXPERIMENT

SCSO CONDITIONS

- Dewar top-plate temperature
- Dewar top-plate temperature controller
- Dewar tilt, X and Y directions
- Dewar tilt-control servo currents, X and Y directions
- Dewar helium vapor pressure
- SCSO room temperature
- SCSO room temperature controller
- SCSO gunn oscillator temperatures (3)

MASER CONDITIONS

- Maser frame temperatures (2)

4. Data Analysis

4.1 Data Preparation

The data discussed here were obtained from the experiment conducted during April 1 - 11, 1978. (A preliminary run for the purpose of checking the experimental conditions was conducted during March 19-28. Prior to the April run, an anti-tilt servo-mechanism was installed on the SCSO dewar, and the outer laboratory air-conditioning was improved.) Data analyses were carried out independently at Stanford University and at SAO. Both analyses included examinations of the linear drift and of the diurnal variation of the frequency. In studying the diurnal variation, the Stanford effort concentrated on use of Fourier transforms of the data,

while the SAO work used regression and correlation techniques on both the frequency data and the time derivative of frequency. Similar results were obtained with the two approaches. In this report we discuss mainly the SAO data analysis.

The four sets of beat period data were transformed into relative frequency changes, f_{12}, f_{13}, f_{15}, and f_{16}. (All frequency differences were divided by the oscillator frequencies and expressed as fractional differences.) Data points that were clearly identified as being spurious were removed and the frequencies were identified at identical twenty-minute intervals using a forty-minute Hanning filter. The four resulting time series were suitably added together to yield the ten frequency difference functions that are possible with five oscillators. These are shown in Figs. 2-11.

The ambient condition data were interpolated to produce time series whose values were in temporal registration with the frequency data. Of the 13 streams of ambient condition data, only three showed behavior that resembled variations in the frequency differences. These three were the vapor pressure of the helium gas in the SCSO dewar and the temperatures of each of the maser cabinets. They are referred to as HP, T5, and T6, respectively, and are shown in Figs. 12 to 14. During the first two days of the experiment the helium vapor pressure (HP) fell rapidly. The SCSO frequencies, particularly that of S2, showed corresponding rapid shifts. During the eleventh day of the experiment the liquid helium level fell below a critical level, causing a change in HP and an abrupt change in the SCSO frequencies. In order to eliminate data that were obviously affected by strong systematic effects, we disregarded the data from the beginning and end of the

experiment, keeping 8 days' of data between days 2.8 and 10.8. (Time is measured in solar days beginning at one minute after midnight on the morning of April 1.)

All subsequent analyses of the data use as input these three ambient-condition time series and four frequency difference time series.

4.2 Linearly Varying Component of Solar Gravitational Potential

As shown in Eq. 5, the solar potential consists primarily of two terms: a diurnal variation with daily peak-to-peak change of approximately 6×10^{-13}, and a linear variation with a daily change of approximately 3×10^{-12}. Because of the relatively large magnitude of the linear term, the existence of a gravitational effect on the oscillators would appear in the oscillator frequency differences primarily as a linear change with time. The linear variations of the frequency differences are examined in this section. A search for a diurnal component ascribable to the solar potential is discussed in section 4.3.

From Figs. 2 to 11 it is apparent that all of the frequency differences, including those for maser-maser and SCSO-SCSO pairs, have relative drifts of up to 3.6×10^{-13} in 8 days, or 4.5×10^{-14} per day. Since the solar potential is varying at the rate of 2.84×10^{-12} per day, we can quickly set an upper limit on the quantity α_{ms} of roughly 1.6×10^{-2} if we ascribe all of the frequency drift to the gravitational potential. This estimate does not, however, take into account non-gravitational systematic effects acting on the oscillators. The effects of the helium vapor pressure and of the maser frame temperatures were removed by performing a multiple function linear regression on each frequency-difference time series. The independent functions used in the regression were the calculated solar gravitational potential U and the

ambient effects appropriate to the particular frequency differences; for example, HP, T_5 and U were regressed on f_{15}; HP and U on f_{13}; T_5, and T_6, and U on f_{56}; and so forth. Of the ten frequency functions, six (written f_{kn}) are frequency differences between dissimilar oscillators (maser-SCSO), and four (written f_{rt}) are differences between similar oscillators (maser-maser and SCSO-SCSO). The regression coefficient, b_{kn}, of U on each of the f_{kn} is proportional to any component of f_{kn} that varies with the gravitational potential U, and thus gives a value for α_{ms}. (Similar oscillators can have no mutual frequency difference induced by U, so the regression coefficients of U on the f_{rt} measure the presence of unidentified systematic effects, or of ambient effects containing linear or diurnal components that were not completely removed by the regression.) The regression coefficients are given in Table III.

TABLE III

REGRESSION COEFFICIENTS OF U ON FREQUENCY DIFFERENCES BETWEEN PAIRS OF OSCILLATORS

OSCILLATORS	REGRESSION COEFFICIENT b_{ij}	STANDARD ERROR of b_{ij}
5-1	1.45×10^{-2}	3.4×10^{-4}
5-2	1.25×10^{-2}	2.4×10^{-4}
5-3	0.57×10^{-2}	3.1×10^{-4}
6-1	1.50×10^{-2}	7.3×10^{-4}
6-2	1.39×10^{-2}	5.9×10^{-4}
6-3	0.67×10^{-2}	4.5×10^{-4}
6-5	0.30×10^{-2}	1.7×10^{-4}
2-1	0.36×10^{-2}	2.6×10^{-4}
3-2	0.58×10^{-2}	3.2×10^{-4}
3-1	0.93×10^{-2}	3.6×10^{-4}

The standard errors of the regression coefficients, which are the errors due to scatter of the data about the regression lines, are at most 7 per cent of the values of the coefficients, while the variations among the coefficients are on the order of magnitude of the coefficients; hence, the errors in determining the individual coefficients (the standard errors) do not significantly affect the variations among coefficients and will be ignored in the following analysis.

Table III shows that the regression coefficients--and thus the relative drift rates--for masers verses SCSOs are all positive (that is, both masers increase in frequency faster than any of the SCSOs), and that the drift rates between dissimilar oscillators are for the most part greater than those between pairs of similar oscillators, indicating that the two groups of oscillators are changing frequency at significantly different rates.

The measurements of frequency differences between dissimilar oscillators constitute a group of experiments, each leading to a value for α_{ms}, from which we wish to determing the mean value $\overline{\alpha}_{ms}$ and its confidence interval. We cannot, however, simply use the six regression coefficients b_{kn} between dissimilar oscillators to estimate $\overline{\alpha}_{ms}$, because these measurements are not independent. Since the frequency data are related by linear superposition, only four of the six coefficients for dissimilar oscillators are statistically independent. For example, the frequency differences f_{51}, f_{52}, f_{61}, and f_{63} produce the differences f_{53} and f_{62}; by linear superposition, therefore, the regression coefficients b_{53} and b_{62} are related to b_{51}, b_{52}, b_{61} and b_{63}. Of the fifteen sets of four coefficients that can be chosen from the six b_{kn}, three sets are not complete in that they do not generate the remaining two coefficients; these sets are (b_{51}, b_{52}, b_{61}, b_{62}) and (b_{52}, b_{53}, b_{62}, b_{63}), and (b_{53}, b_{51}, b_{63}, b_{61}). The remaining twelve sets of coefficients represent different ways of measuring α_{ms}, that is, they can be regarded as twelve possible sets of four independent experiments. The sets are not, however, independent of one another, and we must choose the averaged results of one set to estimate α_{ms}.

Table IV gives the average regression coefficients for the twelve sets of data. The maximum value of $\bar{b}$ is 1.25×10^{-2} and the minimum is 0.99×10^{-2}, the span between these being less than the typical standard error of approximately 0.4×10^{-2}, indicating that our conclusion will not be sensitive to the choice of data set.

TABLE IV

Mean Regression Coefficients for Independent Sets of Dissimilar Oscillators

SET	OSCILLATORS	MEAN REGRESSION COEFFICIENT $\bar{b}$	STANDARD DEVIATION of $\bar{b}$
IV-1	5-1, 6-1, 5-2, 5-3	1.19×10^{-2}	$.43 \times 10^{-2}$
IV-2	5-1, 6-1, 5-2, 6-3	1.22×10^{-2}	$.38 \times 10^{-2}$
IV-3	5-1, 6-1, 6-2, 5-3	1.23×10^{-2}	$.44 \times 10^{-2}$
IV-4	5-1, 6-1, 6-2, 6-3	1.25×10^{-2}	$.39 \times 10^{-2}$
IV-5	5-2, 6-2, 5-3, 5-1	1.17×10^{-2}	$.41 \times 10^{-2}$
IV-6	5-2, 6-2, 5-3, 6-1	1.18×10^{-2}	$.42 \times 10^{-2}$
IV-7	5-2, 6-2, 6-3, 5-1	1.19×10^{-2}	$.36 \times 10^{-2}$
IV-8	5-2, 6-2, 6-3, 6-1	1.20×10^{-2}	$.37 \times 10^{-2}$
IV-9	5-3, 6-3, 5-1, 5-2	0.99×10^{-2}	$.43 \times 10^{-2}$
IV-10	5-3, 6-3, 5-1, 6-2	1.02×10^{-2}	$.46 \times 10^{-2}$
IV-11	5-3, 6-3, 6-1, 5-2	1.00×10^{-2}	$.45 \times 10^{-2}$
IV-12	5-3, 6-3, 6-1, 6-2	1.03×10^{-2}	$.48 \times 10^{-2}$

To estimate an upper bound for $\overline{\alpha}_{ms}$ we use the maximum value for $\overline{b}$ and the maximum standard deviation; thus the maximum value of $\overline{\alpha}_{ms}$ estimated from the linear component of the solar potential is

$$\alpha_{ms}^{\text{linear}} = (1.25 \pm 0.40) \times 10^{-2} \tag{6}$$

The t distribution with three degrees of freedom gives the 95 per-cent confidence interval for $\overline{\alpha}_{ms}^{\text{linear}}$ as

$$0.49 \times 10^{-2} \leq \alpha_{ms}^{\text{linear}} \leq 2.01 \times 10^{-2} \tag{7}$$

Hence with 95 per-cent confidence we estimate the upper bound as

$$\overline{\alpha}_{ms}^{\text{linear}} \leq 2.01 \times 10^{-2} \tag{8}$$

4.3 Diurnal Component of Solar Gravitational Potential

Because the diurnal component of U is far smaller than the linearly varying component, the regression calculation described in Section 4.2 is relatively insensitive to the diurnal component. This was verified by a regression calculation on the frequency data in which the diurnal term was treated separately from the linear term; this yielded no significant diurnal component of f_{ms} at the 95 per-cent confidence level. In order to search for a gravitational effect without being obscured by long-term drifts, we used advanced time-series analysis techniques to examine the data for the presence of a diurnal variation in phase with the solar gravitational potential.

The frequency differences of Figures 2 to 11 show substantial long-period fluctuations with durations from fractions of days to several days. This non-stationary behavior is characteristic of noise produced by a first-order auto-regressive process, that is, one with the ability to integrate past effects. The noise is far from white; rather, it has a distinctly red, or low frequency, character. In order to be able to detect shorter-period variations, we removed the low frequency noise by transforming the frequency functions with the inverse of the auto-regressive process, namely, the time derivative. Figs. 15 to 24 show the time derivatives of the frequency series; short-term variations with periods of approximately one-half day are clearly visible. (We will, henceforth, refer to these time derivatives of the frequency series as derivative series or frequency derivatives.) The auto-correlation functions of the frequency derivatives, as well as Fourier transforms of the frequency data calculated at Stanford University, showed that the dominant periodicity of several of the frequency series was approximately

0.51 days. We confirmed these period estimates with greater precision by the use of super-resolution, a non-linear least squares regression technique in which a trigometric function $A \cos (\frac{2\pi}{T} t + \phi)$ is fitted to the data by adjusting the amplitude (A), period (T), and phase (ϕ) of the function. The period of the semi-diurnal perturbation was determined by this method to be $0.507 \pm .002$ solar days. This is significantly longer than half a solar day and suggests the effect of the lunar gravitational tide.

Possible mechanisms of lunar perturbation are changes in the local gravitational acceleration g (the effect that causes the ocean tides), and variations in the atmospheric pressure p, which is affected by the variation in g, resulting in the atmospheric tides. To determine the source of the perturbation we cross-correlated the derivatives of the frequency differences with the time derivative of the calculated value of local g and with the derivative of the barometric pressure measured at Palo Alto during the experiment. The closest correlation was between the frequency derivative and the barometric pressure derivative. The barometric pressure is shown in Fig. 25; its time derivative, $\dot{p}$, together with that of a typical frequency derivative series, is shown in Fig. 26.

To search for the presence of a solar diurnal component in the frequency derivatives, we first regressed $\dot{p}$ on the $\dot{f}_{ij}$, obtaining the regression coefficients of Table V.

TABLE V

REGRESSION COEFFICIENTS FOR BAROMETRIC PRESSURE DERIVATIVE $\dot{p}$ REGRESSED ON FREQUENCY DERIVATIVES $\dot{f}_{ij}$

OSCILLATOR PAIR	REGRESSION COEFFICIENT x 10^{14} $(\text{INCH Hg})^{-1}$
1-5	12.0
2-5	6.4
3-5	- 8.1
1-6	33.8
2-6	25.0
3-6	18.1
5-6	22.6
1-2	9.3
2-3	7.0
1-3	16.1

Note that for oscillator pairs involving maser P6, the regression coefficients, which measure the sensitivity of the oscillators' frequencies to changes in barometric pressure, are substantially larger than for most other oscillator pairs. The source of this difference, and its possible effect on the results of the experiment, are discussed in Section 5.2. Using these coefficients we then removed the effect of $\dot{p}$ from the $\dot{f}_{ij}$, yielding residual frequency derivatives $\dot{F}_{ij}$. $\dot{U}$ was then regressed on the residuals to determine regression coefficients a_{ij}. (Because the functions in the regression were adjusted to zero mean, $\dot{U}$ contains only a contribution from the derivative of the diurnal component.) The regression coefficients a_{kn} for dissimilar oscillators, which give values for α_{ms}, are listed in Table VI.

TABLE VI

REGRESSION COEFFICIENTS OF $\dot{U}$ ON RESIDUAL FREQUENCY DERIVATIVES (BAROMETRIC PRESSURE REMOVED)

OSCILLATORS	REGRESSION COEFFICIENT a_{ij}
1-5	$.48 \times 10^{-2}$
2-5	$.59 \times 10^{-2}$
3-5	$.62 \times 10^{-2}$
1-6	$.99 \times 10^{-2}$
2-6	1.04×10^{-2}
3-6	1.37×10^{-2}
2-1	$.04 \times 10^{-2}$
3-2	$.21 \times 10^{-2}$
3-1	$.17 \times 10^{-2}$
5-6	$.52 \times 10^{-2}$

As discussed in Section 4.2, only certain sets of four of the six coefficients between dissimilar oscillators can be regarded as independent measurements of α_{ms}. The twelve possible sets of independent dissimilar oscillator pairs, and the mean regression coefficient determined by each set, are given in Table VII.

TABLE VII

MEAN REGRESSION COEFFICIENTS a_{kn} OF U ON F_{kn} FOR INDEPENDENT SETS OF DISSIMILAR OSCILLATORS

SET	OSCILLATORS	COEFFICIENT a_{kn}	DEVIATION OF a_{kn}
1	1-5, 1-6, 2-5, 3-5	$.67 \times 10^{-2}$	$.22 \times 10^{-2}$
2	1-5, 1-6, 2-5, 3-6	$.86 \times 10^{-2}$	$.41 \times 10^{-2}$
3	1-5, 1-6, 2-6, 3-5	$.78 \times 10^{-2}$	$.28 \times 10^{-2}$
4	1-5, 1-6, 2-6, 3-6	$.97 \times 10^{-2}$	$.37 \times 10^{-2}$
5	2-5, 2-6, 3-5, 1-5	$.68 \times 10^{-2}$	$.25 \times 10^{-2}$
6	2-5, 2-6, 3-5, 1-6	$.81 \times 10^{-2}$	$.24 \times 10^{-2}$
7	2-5, 2-6, 3-6, 1-5	$.87 \times 10^{-2}$	$.41 \times 10^{-2}$
8	2-5, 2-6, 3-6, 1-6	1.00×10^{-2}	$.32 \times 10^{-2}$
9	3-5, 3-6, 1-5, 2-5	$.77 \times 10^{-2}$	$.41 \times 10^{-2}$
10	3-5, 3-6, 1-5, 2-6	$.88 \times 10^{-2}$	$.41 \times 10^{-2}$
11	3-5, 3-6, 1-6, 2-5	$.89 \times 10^{-2}$	$.37 \times 10^{-2}$
12	3-5, 3-6, 1-6, 2-6	1.00×10^{-2}	$.31 \times 10^{-2}$

The maximum value for $\bar{a}_{kn}$ is 1.00×10^{-2} and the maximum value for the standard deviation of a_{kn} is $.41 \times 10^{-2}$; thus the maximum value of $\overline{\alpha}_{ms}$ estimated from the diurnal component of the solar potential is

$$\overline{\alpha}_{ms}^{\text{diurnal}} = (1.00 \pm .41) \times 10^{-2} \qquad (9)$$

The 95 per-cent confidence interval for $\overline{\alpha}_{ms}^{\text{diurnal}}$ is

$$.35 \times 10^{-2} \leq \overline{\alpha}_{ms}^{\text{diurnal}} \leq 1.65 \times 10^{-2} \qquad (10)$$

and the estimated upper limit for $\overline{\alpha}_{ms}^{\text{diurnal}}$ is

$$\alpha_{ms}^{\text{diurnal}} \leq 1.65 \times 10^{-2} \qquad (11)$$

5. DISCUSSION OF RESULTS

5.1 Linear Drift of Frequency

We have seen that the masers have frequency drift rates of several parts in 10^{14} per day relative to the SCSOs, with the maser frequencies consistently increasing with respect to the SCSOs. If all of this drift is ascribed to the solar gravitational potential one concludes, as in Section 4.1, that α_{ms} has a value of (1 to 2) x 10^{-2}. However, frequency standards are often subject to long-term systematic drifts; in particular, it has recently been found at SAO and at other laboratories [7] that some hydrogen masers have slow upward drifts in frequency at a rate of up to 1 to 2 parts in 10^{14} over time spans of many months. This is believed to be due to settling of the ground joints of their Cervit[8] resonant cavities. Over the year prior to this experiment, P6's resonant cavity decreased in length at a rate corresponding to a change in output frequency of 1.6 x 10^{-14}/day. (This change was compensated by retuning the maser periodically, that is, adjusting the cavity resonance frequency so that the output frequency is independent of the hydrogen beam intensity.[2] This procedure returned the output frequency to its canonical value; between tuning, however, the frequency increased approximately linearly.) Data on maser P5's cavity frequency drift are fragmentary; however, Table III shows that the 5-6 regression coefficient, and hence the drift rate between masers P5 and P6, is small compared to those of other oscillator pairs, leading to the conclusion that P5's frequency had a long-term behavior similar to that of P6. It appears, then, that the frequencies of both P5 and P6 drifted upward at rates of approximately 1 to 2 x 10^{-14}/day during the experiment due to resonant cavity deformation. A spontaneous frequency drift of 1.6 x 10^{-14}/day (P6's drift rate) due to the masers contributes to α_{ms} approximately 0.54 x 10^{-2},

which is 40 percent of the value of $\bar{\alpha}_{ms}$ obtained in Eq. 6. Correcting $\alpha_{ms}^{\text{linear}}$ for this cavity-induced drift gives

$$\bar{\alpha}_{ms}^{\text{linear}} \text{ (corrected)} = (0.71 \pm 0.48) \times 10^{-2} \qquad (12)$$

and the upper bound for the 95 percent confidence interval becomes

$$\bar{\alpha}_{ms}^{\text{linear}} \text{ (corrected)} \leq 1.47 \times 10^{-2}. \qquad (13)$$

5.2 Diurnal Frequency Variations

As shown by the regression coefficients of Table V, changes in barometric pressure affect all of the frequency differences, particularly those involving SCSO S1 or maser P6. This is caused by the physical construction of the oscillators. The SCSOs' barometric sensitivities arise from the fact that they are suspended by waveguides from a plate covering their dewar; changes in barometric pressure deflect the plate, which tilts the SCSO cavities, causing changes in cavity dimensions that alter the cavity resonance frequencies. (9)

The masers' barometric sensitivities were measured in a pressure chamber at the Jet Propulsion Laboratory after this experiment. P6's sensitivity was found to be approximately 3×10^{-13}/inch Hg, which is consistent with the results shown in Table V and is far greater than the sensitivities of other masers. When P6 was subsequently disassembled, the anamalous barometric sensitivity was found to have been due to a mechanical interference within the maser, which was then corrected. In contrast, P5 has had no detectable barometric sensitivity in tests at SAO; measurement uncertainty places an upper bound of approximately 8×10^{-15}/inch Hg on P5's sensitivity.

The oscillators' barometric sensitivities can affect the estimation of the diurnal solar effect in the following way. The local variation of g, and thus the atmospheric tides, have a diurnal component in addition to the dominant semidiurnal term. (10) Because the regression analysis does not yield a perfect fit of the barometric pressure derivative $\dot{p}$ to the frequency derivatives $\dot{f}_{ij}$, some of the

diurnal variation due to the pressure remains in the frequency residuals $\dot{F}_{ij}$ after removal of $\dot{p}$. Residuals with large remaining diurnal pressure variations may then have high correlations with $\dot{U}$, leading to high estimations for α_{ms}. This is suggested by Table VI: the regression coefficients a_{k6} (k = 1,2,3) for P6-SCSO pairs are approximately twice as large as the a_{k5}. However, the regression coefficients for similar oscillators contradict the notion that residual pressure-induced diurnal variations are the major source of correlation between the frequency residuals and the solar gravitational potential. Although the barometric sensitivities for SCSO-SCSO pairs are at least as large as those for P5-SCSO frequency differences, the a_{rt} for SCSO-SCSO frequency residuals are less than half the magnitudes of the a_{k5}. Also, a_{56} has the same magnitude as the a_{k5} even though $\dot{f}_{56}$ has a much larger sensitivity than do P5-SCSO frequency differences.

This behavior can be explained by the effect of the maser room air temperature, which, as shown in Figs. 13 and 14, has strong diurnal variations. These variations are due to the daily changes of outside air temperature, which are imperfectly compensated for by the laboratory temperature control system. (The SCSOs were held at a constant temperature by the dewar and by careful temperature control of the inner laboratory room.) The effect of maser temperature was not removed in the analysis of the diurnal variation, primarily because the temperature functions are not orthogonal to the solar potential and thus could not be removed unambiguously by a regression technique. The mechanical interference in maser P6 that caused its anomalously large barometric sensitivity was capable of producing a large frequency sensitivity to ambient temperature, resulting in large correlations between $\dot{U}$ and the

frequency residuals involving P6. Because P5 and P6 experienced almost identical ambient temperature variations, their frequency difference would be less affected by temperature than would P6-SCSO frequency differences. This would account for the smaller value of a_{56} compared to a_{k6}. The effect of temperature could properly be removed by measuring the masers' temperature sensitivities in a thermally-controlled chamber to determine the transfer function between ambient temperature and maser frequency. By applying this transfer function to the maser temperatures measured during the experiment, the temperature effect could be removed as a calibration, rather than by means of an adjustable parameter regression. This technique would minimize the liklihood of confusing the effect of temperature with a diurnal frequency variation due to the solar gravitational potential.

5.3 CONCLUSION

The results of this experiment are consistent with the predictions of metric theories of gravitation, with the maximum deviation of α_{ms} from zero being

$$\alpha_{ms} \leq 2.01 \times 10^{-2}$$

This limit is the largest value of the upper bound of the 95 percent confidence interval estimated from the frequency data uncorrected for long-term frequency drifts. After correction for cavity-induced maser frequency drift, the frequency data give $\alpha_{ms}^{\text{linear (corrected)}} \leq 1.47 \times 10^{-2}$, while the diurnal component with barometric pressure sensitivity removed gives $\alpha_{ms}^{\text{diurnal}} \leq 1.65 \times 10^{-2}$.

REFERENCES

1. Will, C.M., Metrologia 13, 95 (1977).

2. Kleppner, D., et. al., Physics Rev. A 138, 972 (1965).
Levine, M.W., R.F.C. Vessot, E. Mattison, G. Nystrom, T. Hoffman, and E. Blomberg, Proc. 31st Ann. Freq. Control Symp., USAERADCOM, Ft. Monmouth, N.J. 07703, May, 1977, p. 525. Published by Electronic Industries Association, Washington, D.C. 20006.

3. Stein, S.R., Proc. 29th Ann. Freq. Control Symposium, USAERADCOM Ft. Monmouth, N.J. 07703, May, 1975, p. 321. Published by Electronic Industries Association, Washington, D.C. 20006.

4. Lightman, A.P., and D.L. Lee, Physics Rev. D 8, 364 (1973).

5. Berger, P., Boston University, Boston, Ma. Private Communication.

6. Farrell, B.F., E.M. Mattison, and R.F.C. Vessot, Proc. 34th Ann. Freq. Control Symp., USAERADCOM, Ft. Monmouth N.J. 07703, May, 1980 (to be published).

7. Kirk, A., Jet Propulsion Laboratory, Pasadena, Ca. Private Communication.

8. Trademark of Owens Illinois Corporation.

9. Turneaure, J.P., Stanford University, Palo Alto, Ca. Private Communication.

10. Melchior, Paul, The Tides of the Planet Earth, Pergamon Press, Oxford (Eng.), 1978

FIGURE CAPTIONS

1. Block diagram of oscillator frequency comparison system.

2-11. Relative frequency differences between pairs of oscillators during experiment.

12. Helium vapor pressure in SCSO dewar during experiment.

13. Temperature of outer frame of maser P5 during experiment.

14. Temperature of outer frame of maser P6 during experiment.

15-24. Time derivatives of frequency differences between pairs of oscillators during experiment.

25. Barometric pressure at Palo Alto, Ca. during experiment.

26. Time derivative of barometric pressure and time derivative of frequency difference between maser P6 and SCSO S1 during experiment.

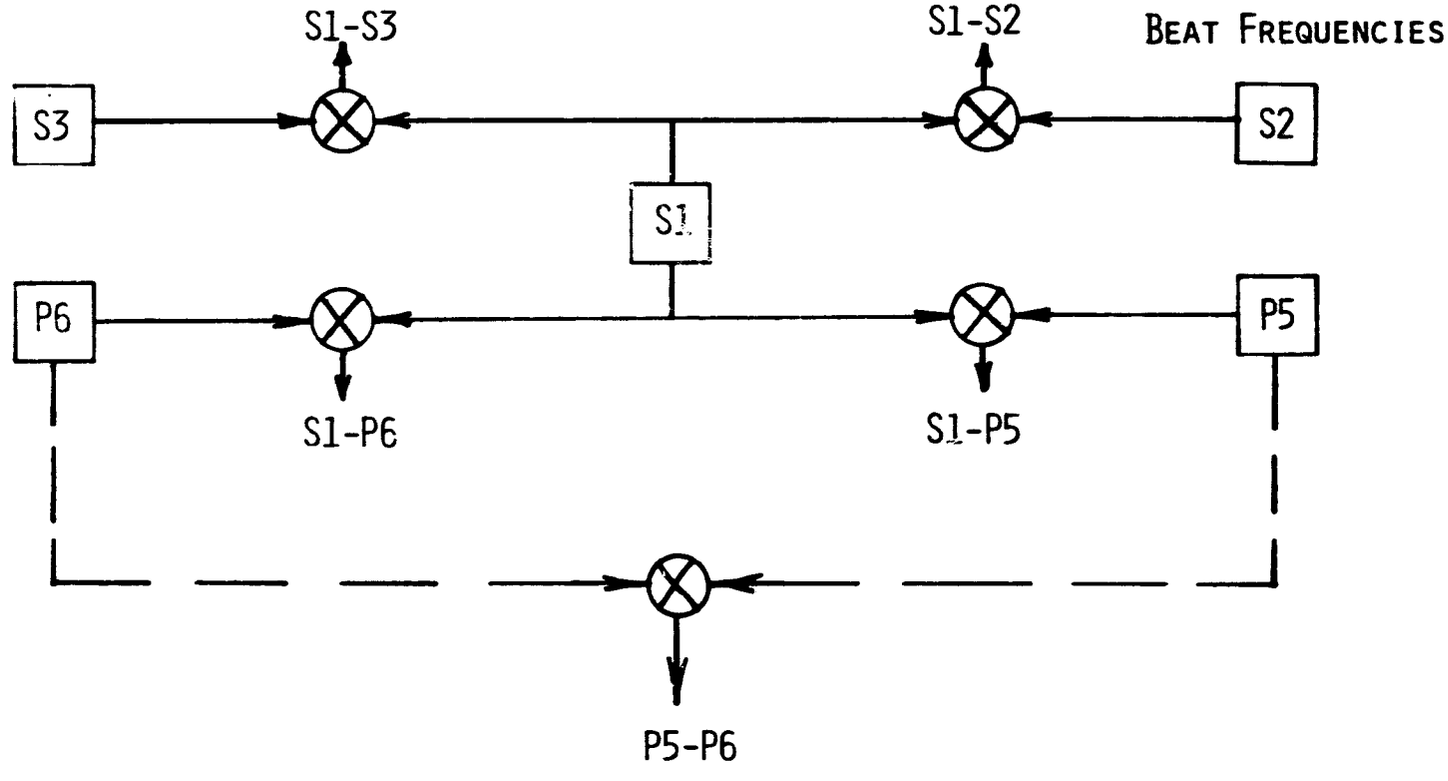

FIGURE 1

Change in relative difference frequency, $\frac{\Delta f}{f} = \frac{\Delta (f_i - f_j)}{f_o}$

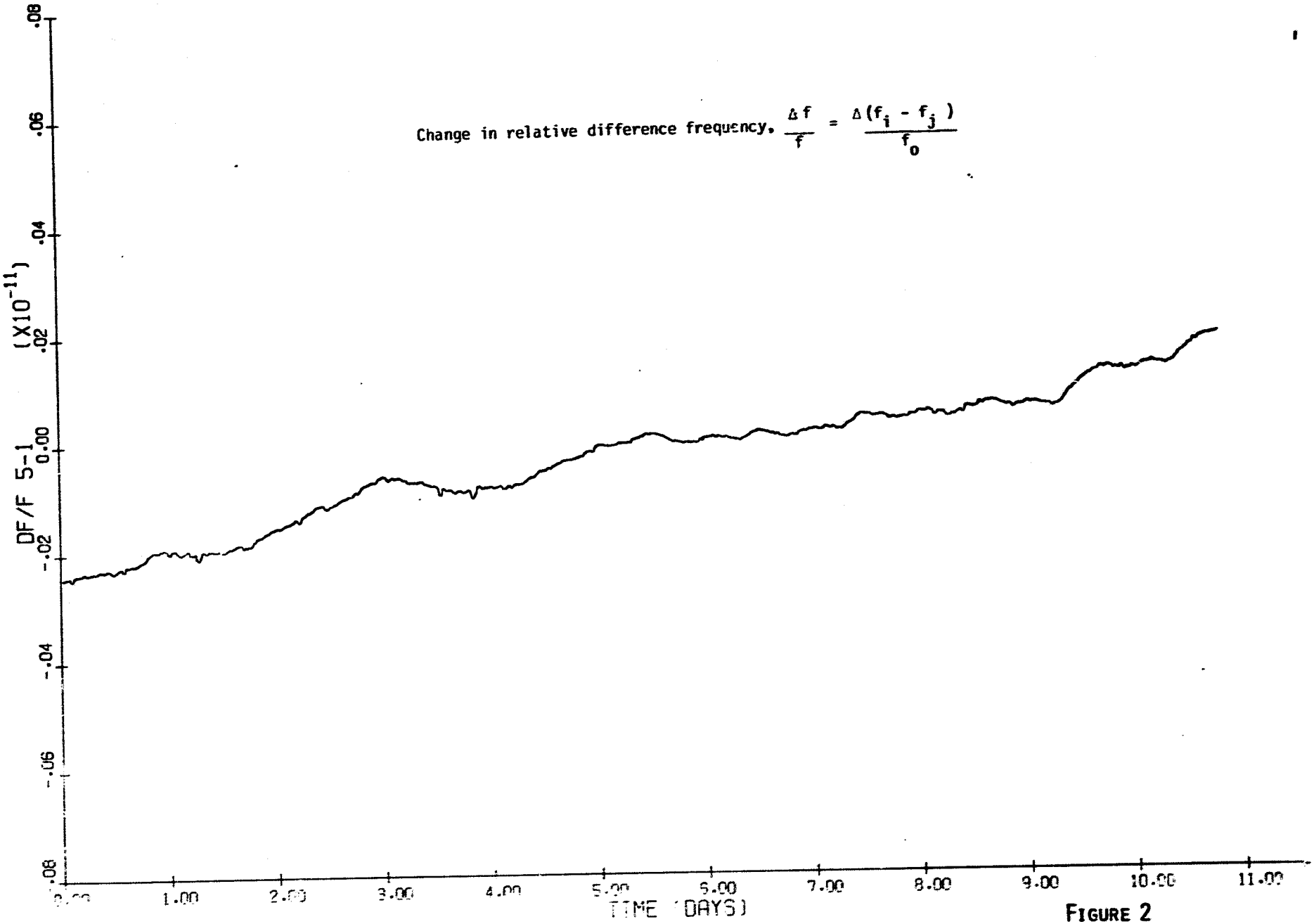

FIGURE 2

Change in relative difference frequency, $\frac{\Delta f}{f} = \frac{\Delta (f_i - f_j)}{f_o}$

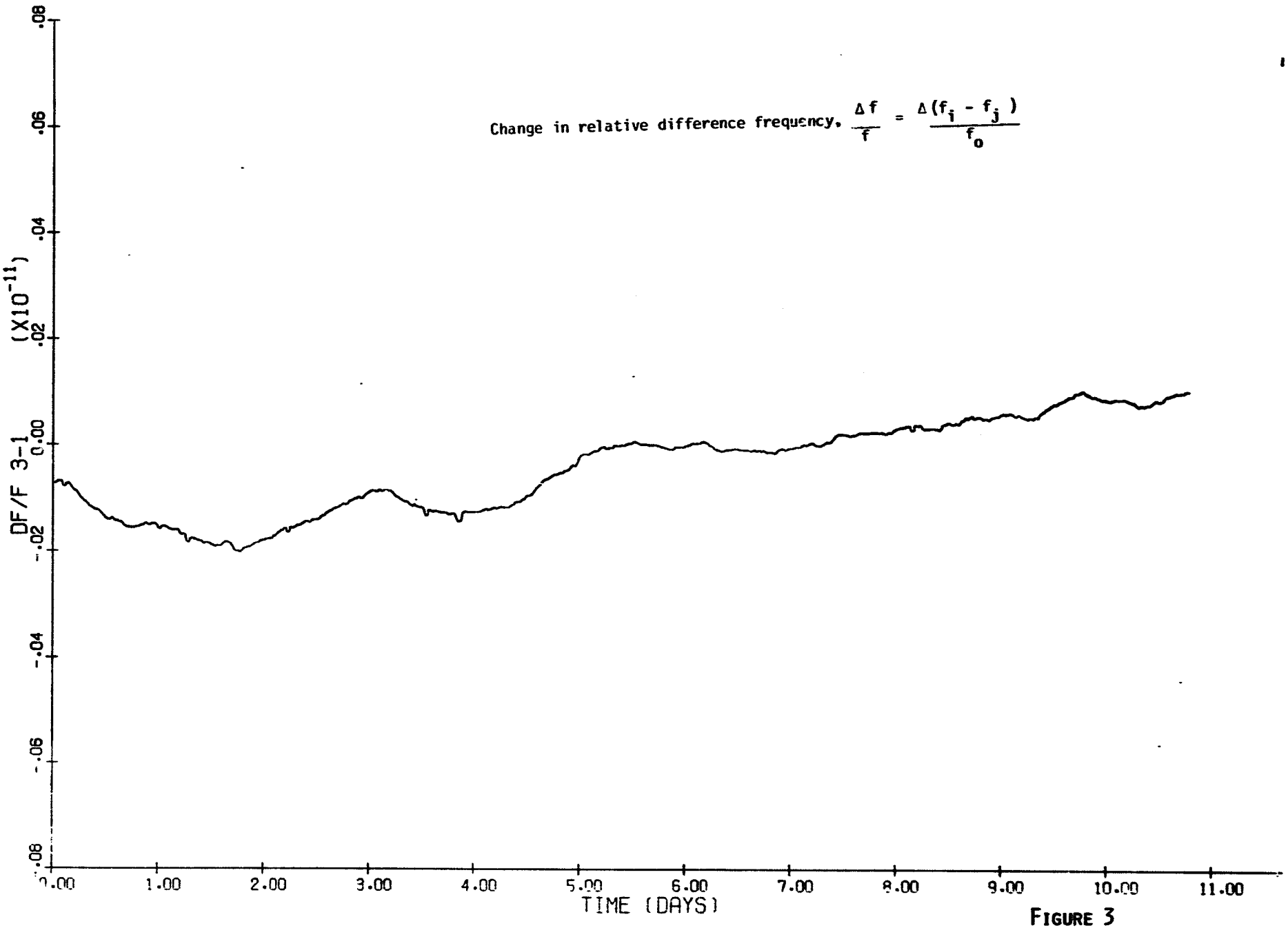

FIGURE 3

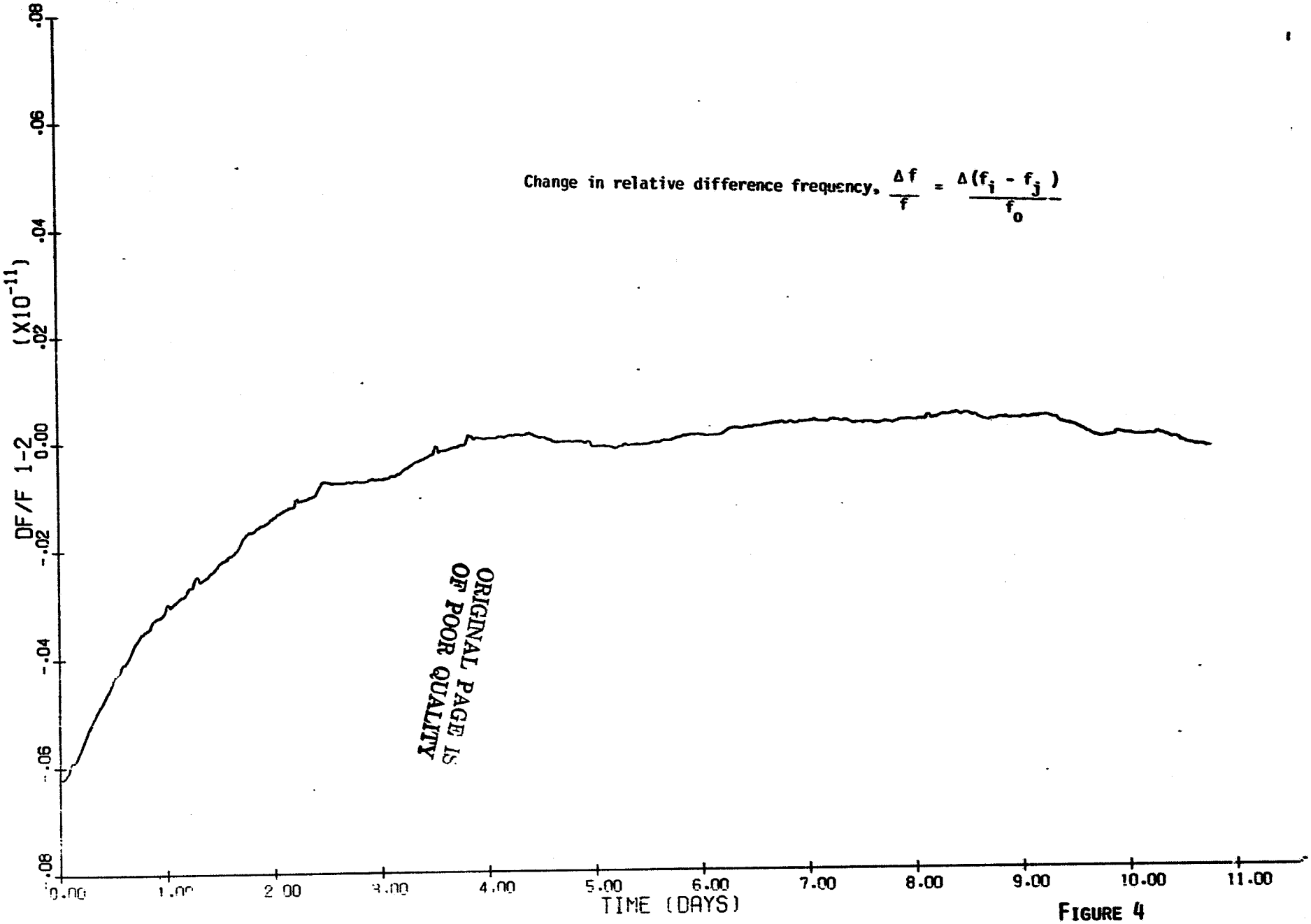

FIGURE 4

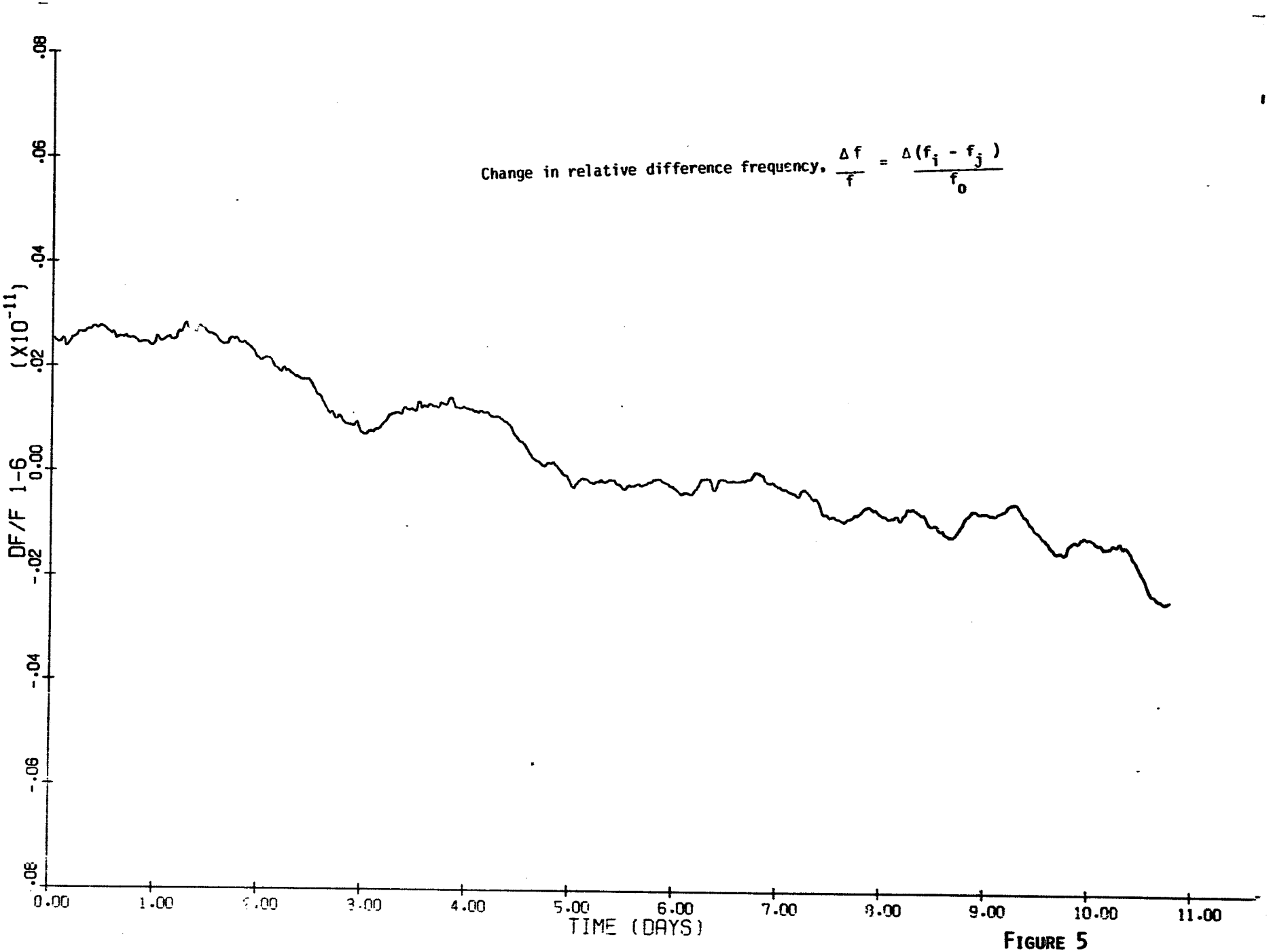
Change in relative difference frequency, $\frac{\Delta f}{f} = \frac{\Delta (f_i - f_j)}{f_0}$
DF/F 1-6 (X10^{-11})
.08
.06
.04
.02
0.00
-.02
-.04
-.06
-.08
0.00
1.00
2.00
3.00
4.00
5.00
6.00
7.00
8.00
9.00
10.00
11.00
TIME (DAYS)

FIGURE 5

Change in relative difference frequency, $\frac{\Delta f}{f} = \frac{\Delta (f_i - f_j)}{f_o}$

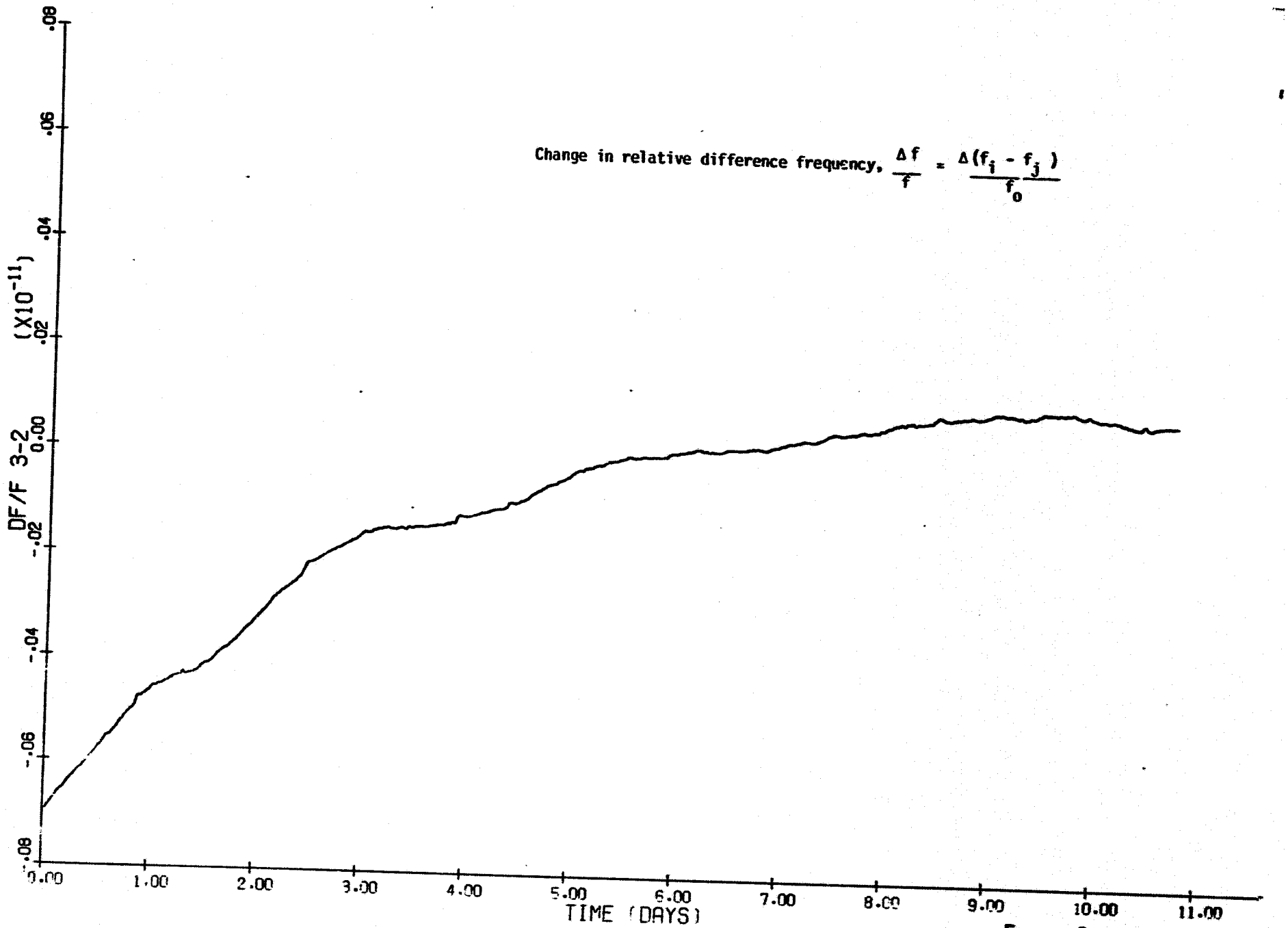

FIGURE 6

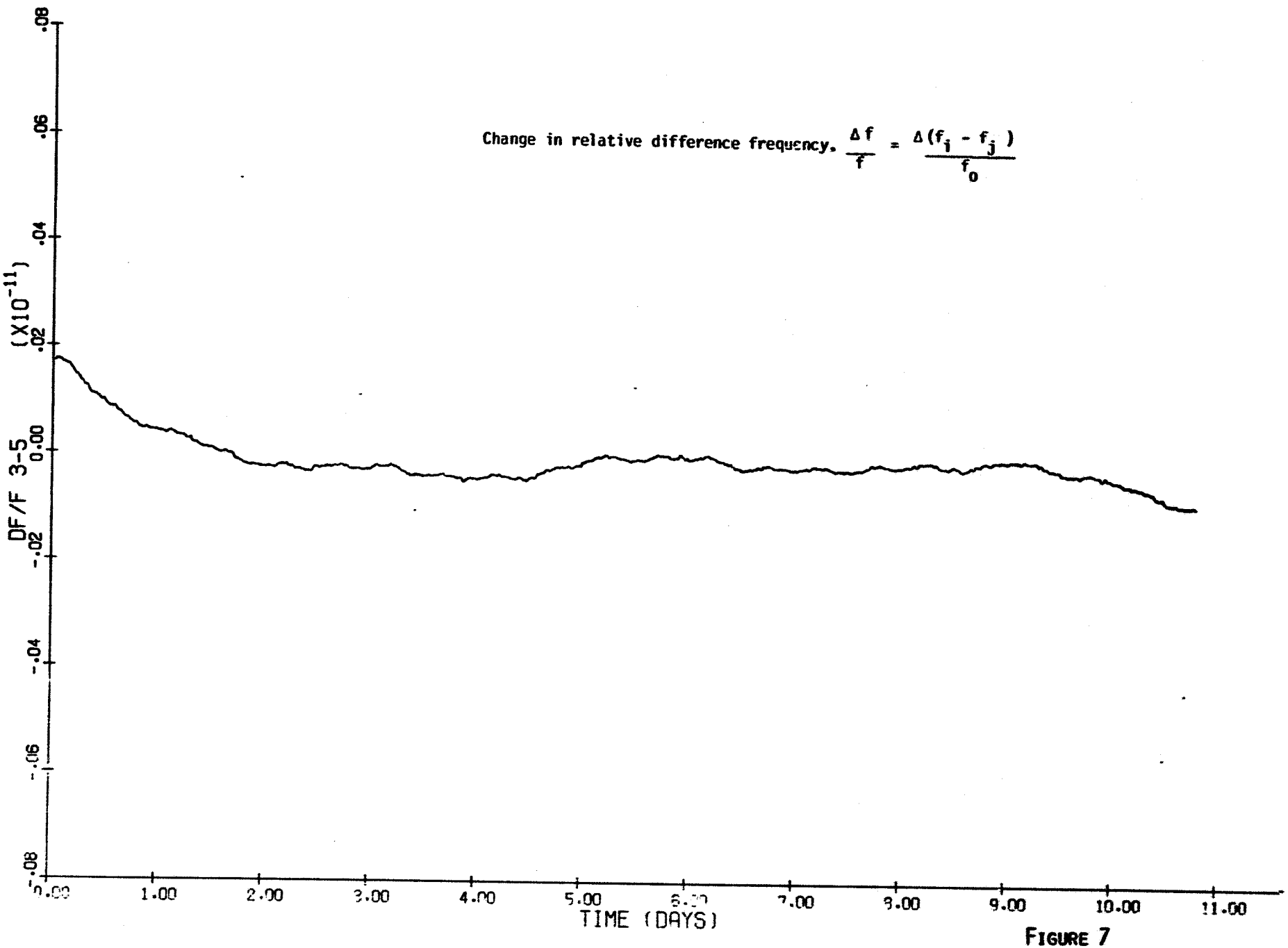
Change in relative difference frequency, $\frac{\Delta f}{f} = \frac{\Delta (f_i - f_j)}{f_o}$
DF/F 3-5 (X10^{-11})
.08
.06
.04
.02
0.00
-.02
-.04
-.06
-.08
1.00
2.00
3.00
4.00
5.00
9.00
10.00
11.00
TIME (DAYS)

FIGURE 7

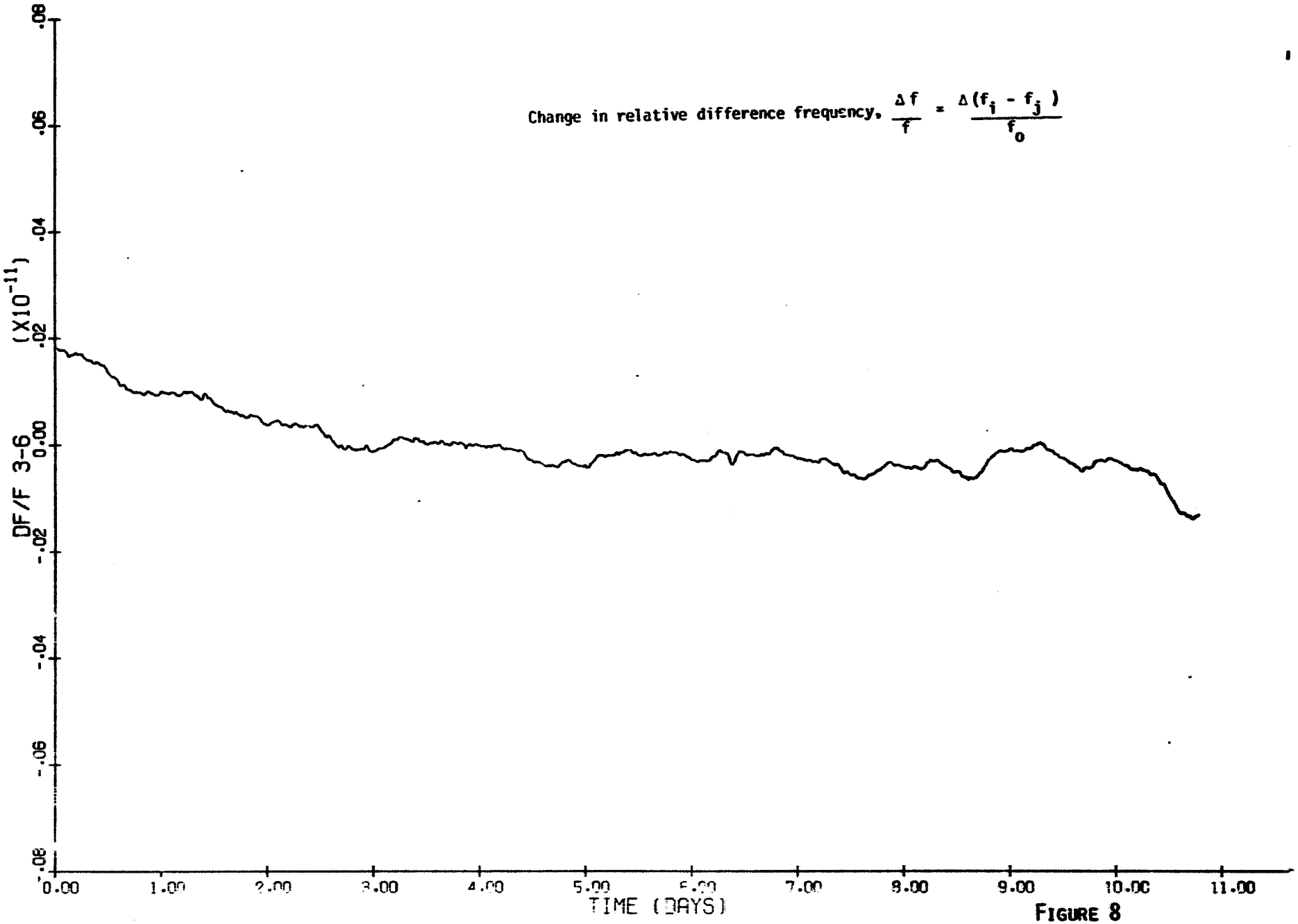
Change in relative difference frequency, $\frac{\Delta f}{f} = \frac{\Delta (f_i - f_j)}{f_o}$
DF/F 3-6 (X10^{-11})
.08
.06
.04
.02
0.00
-.02
-.04
-.06
-.08
0.00
1.00
2.00
3.00
4.00
5.00
7.00
8.00
9.00
10.00
11.00
TIME (DAYS)

FIGURE 8

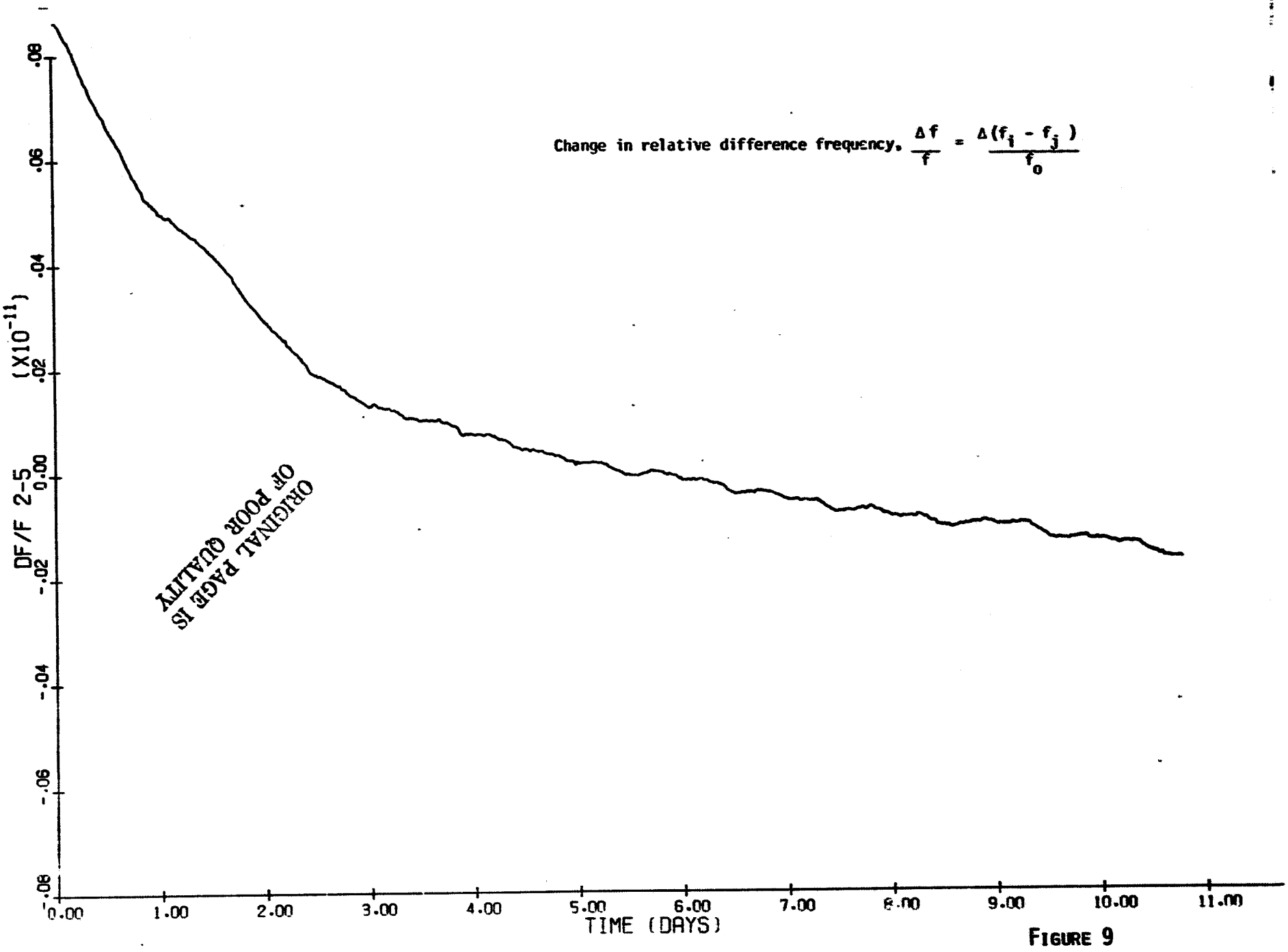
Change in relative difference frequency, $\frac{\Delta f}{f} = \frac{\Delta(f_i - f_j)}{f_0}$
DF/F 2-5 (X10^{-11})
.08
.06
.04
.02
0.00
-.02
-.04
-.06
-.08
ORIGINAL PAGE IS OF POOR QUALITY
0.00
1.00
2.00
3.00
4.00
5.00
6.00
7.00
8.00
9.00
10.00
11.00
TIME (DAYS)

FIGURE 9

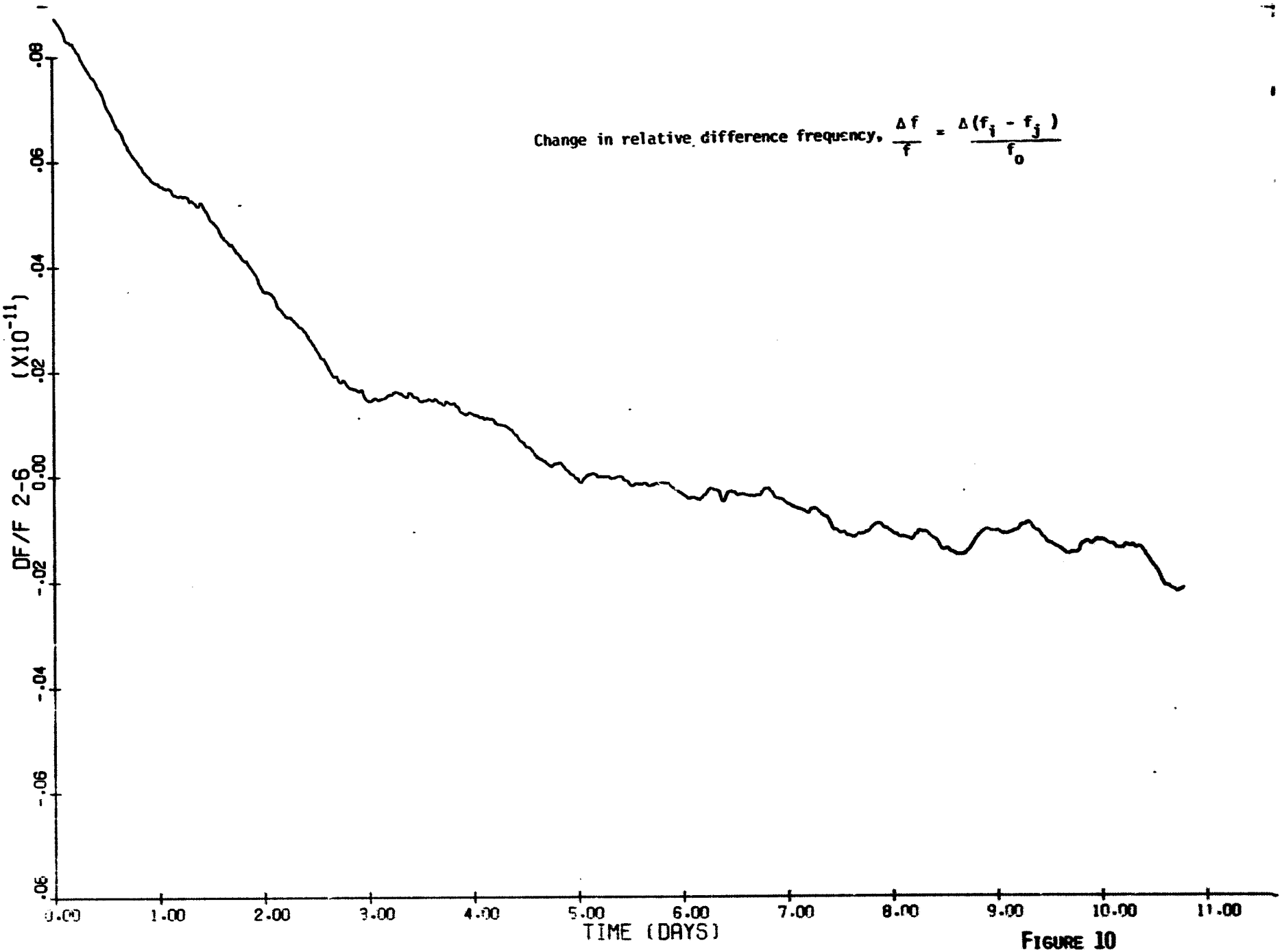
Change in relative difference frequency, $\frac{\Delta f}{f} = \frac{\Delta (f_i - f_j)}{f_o}$
DF/F 2-6 (X10^{-11})
.08
.06
.04
.02
0.00
-.02
-.04
-.06
.06
0.00
1.00
2.00
3.00
4.00
5.00
6.00
7.00
8.00
9.00
10.00
11.00
TIME (DAYS)

FIGURE 10

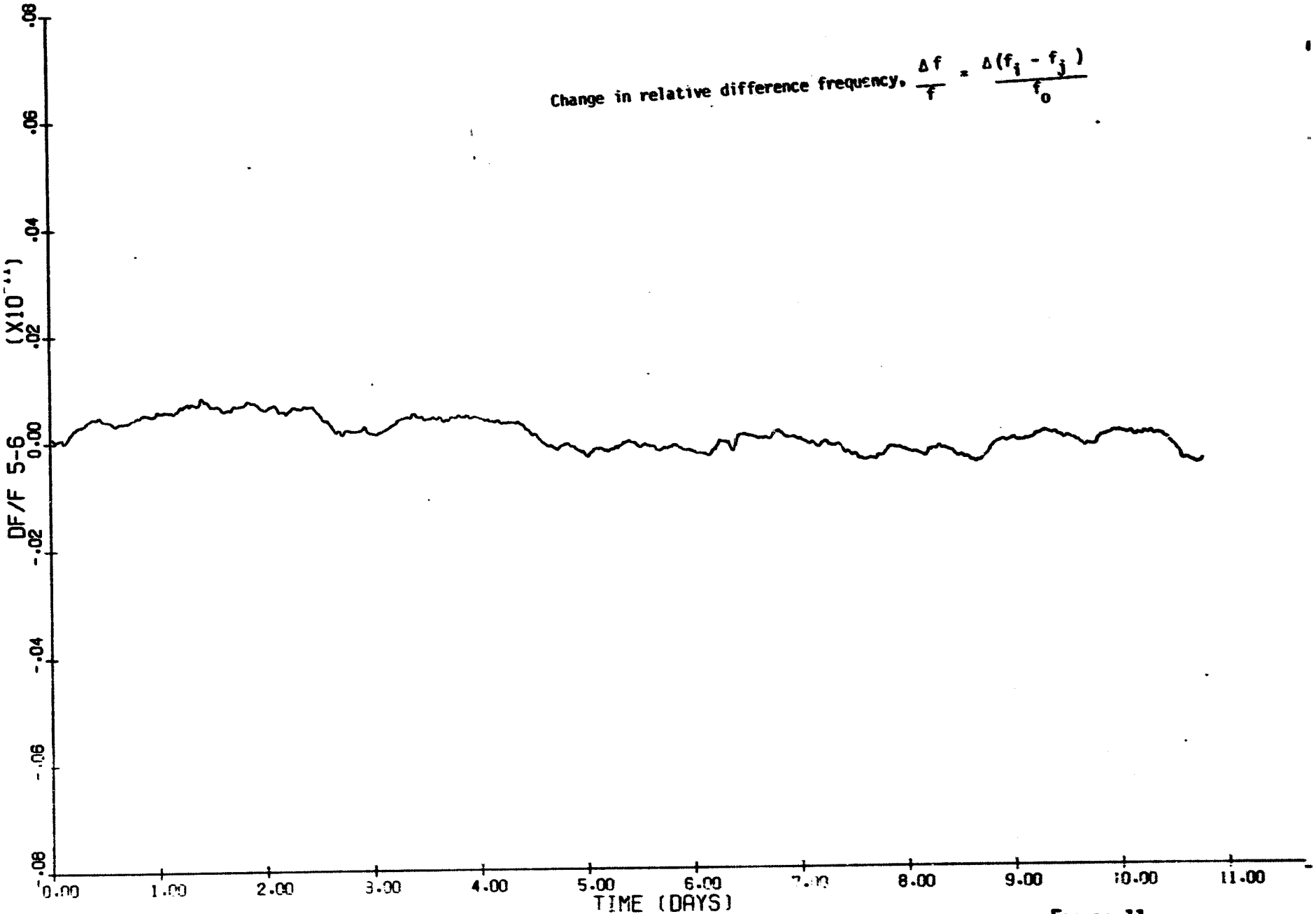
Change in relative difference frequency, $\frac{\Delta f}{f} = \frac{\Delta(f_i - f_j)}{f_o}$
DF/F 5-6 (X10⁻¹⁴)
.08
.06
.04
.02
0.00
-.02
-.04
-.06
-.08
0.00
1.00
2.00
3.00
4.00
5.00
6.00
8.00
9.00
10.00
11.00
TIME (DAYS)

FIGURE 11

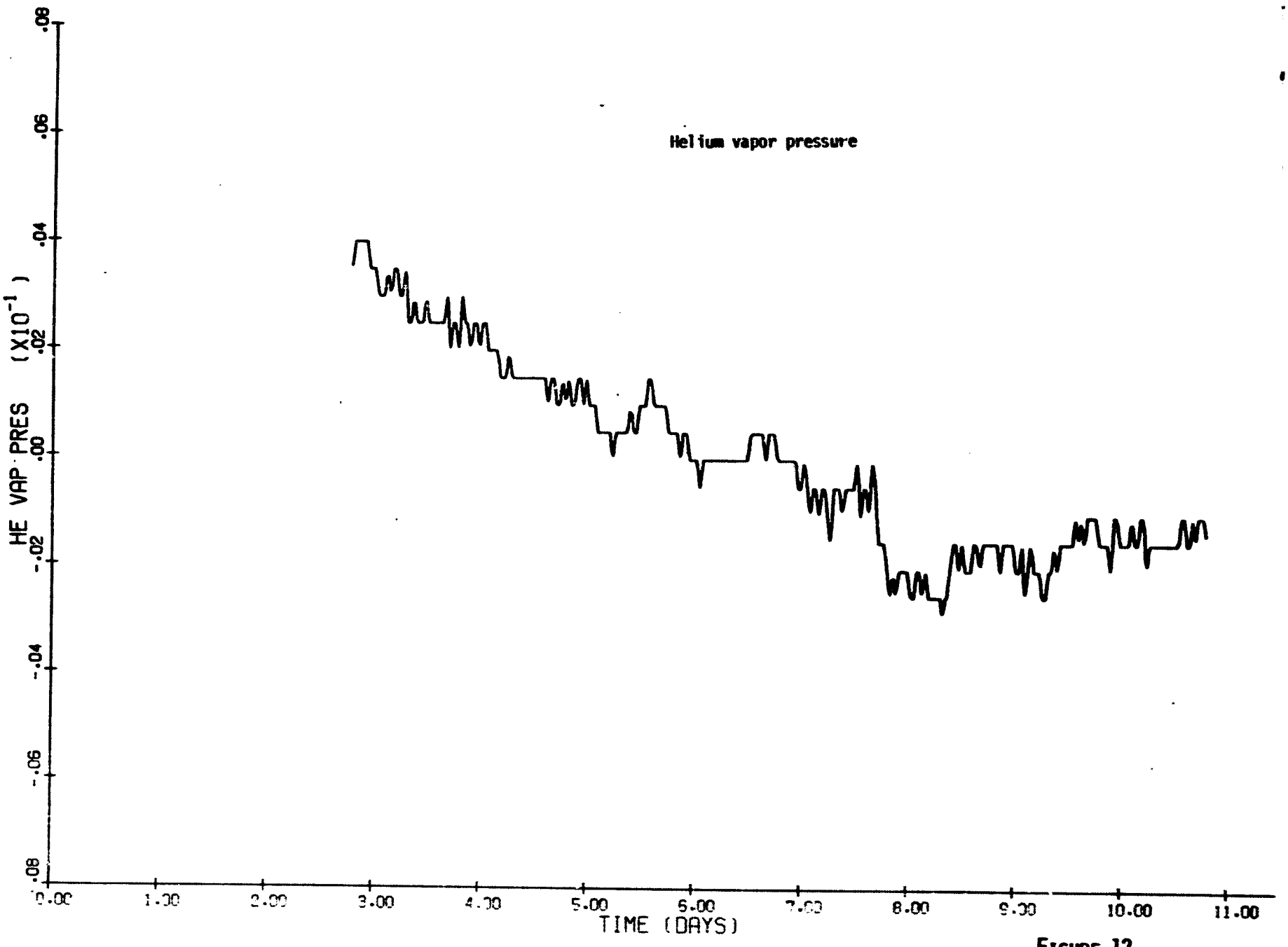
Helium vapor pressure
HE VAP PRES (X10^{-1})
.08
.06
.04
.02
.00
-.02
-.04
-.06
-.08
0.00
1.00
2.00
3.00
4.00
5.00
6.00
7.00
8.00
9.00
10.00
11.00
TIME (DAYS)

FIGURE 12

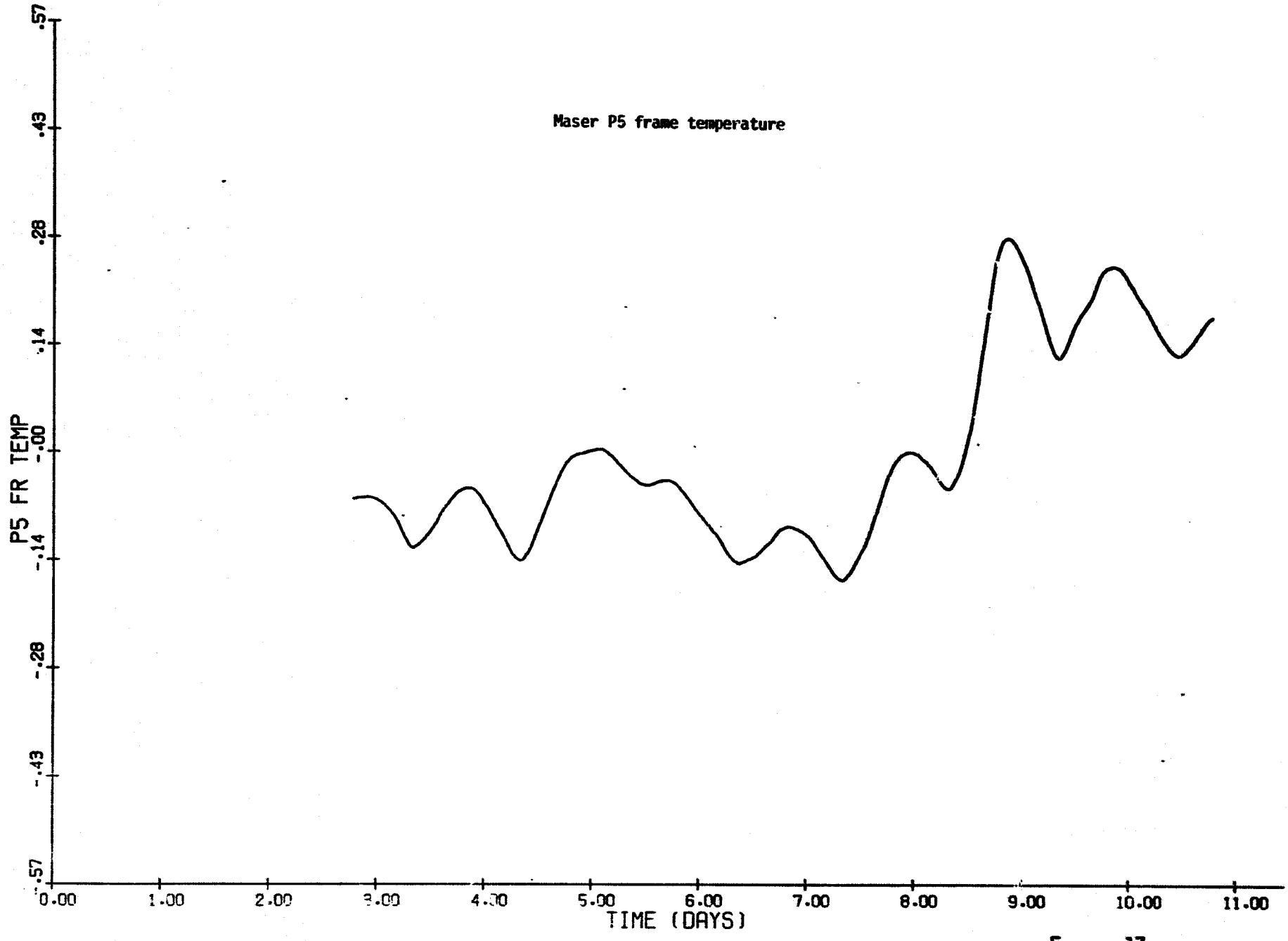
Maser P5 frame temperature
P5 FR TEMP
.57
.43
.28
.14
-.00
-.14
-.28
-.43
-.57
0.00
1.00
2.00
3.00
4.00
5.00
6.00
7.00
8.00
9.00
10.00
11.00
TIME (DAYS)

FIGURE 13

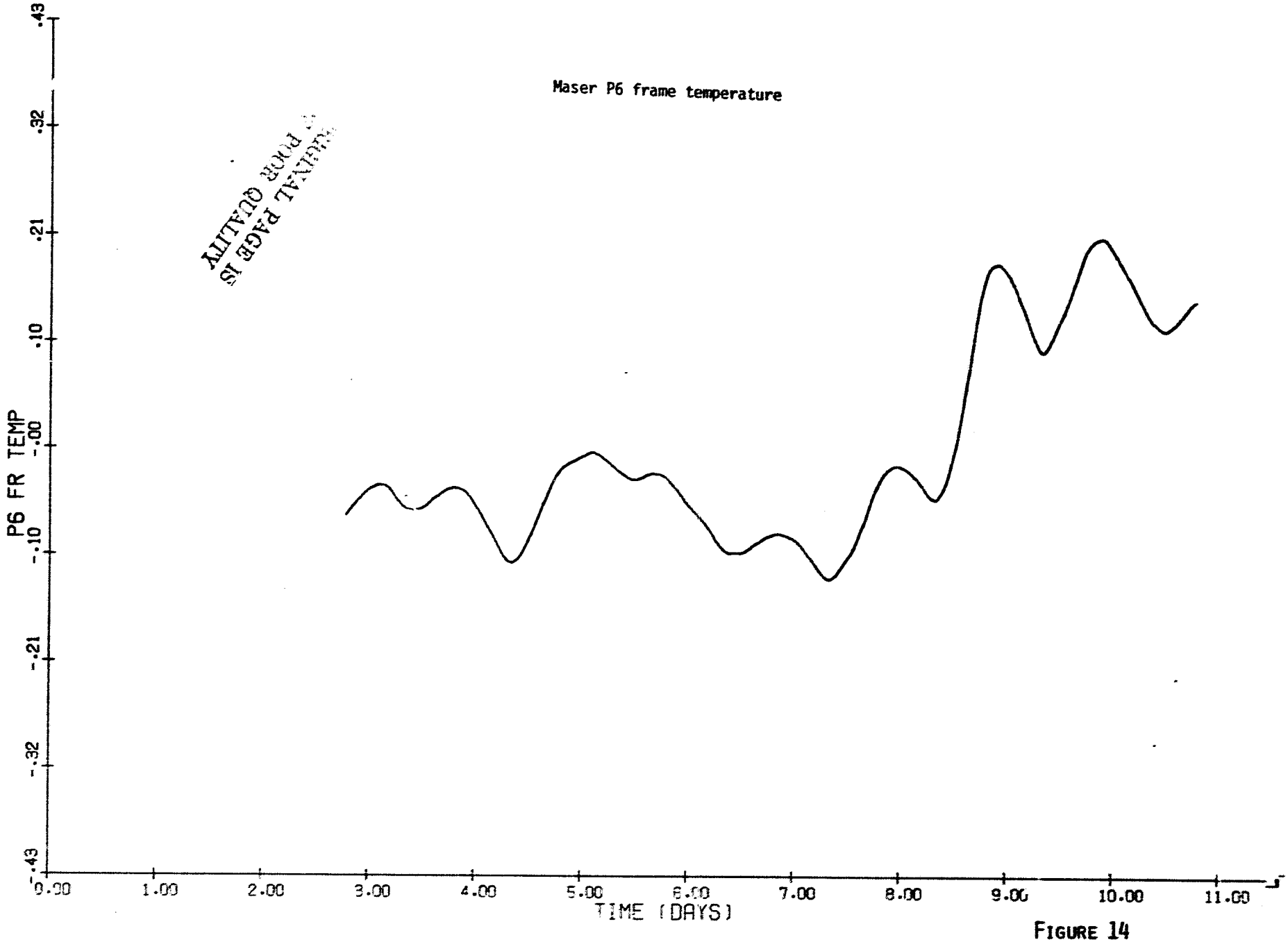
Maser P6 frame temperature
ORIGINAL PAGE IS
OF POOR QUALITY
P6 FR TEMP
.43
.32
.21
.10
-.00
-.10
-.21
-.32
-.43
0.00
1.00
2.00
3.00
4.00
5.00
6.00
7.00
8.00
9.00
10.00
11.00
TIME (DAYS)

FIGURE 14

Time derivative of frequency difference, $\frac{d}{dt}\left(\frac{\Delta f}{f}\right)$

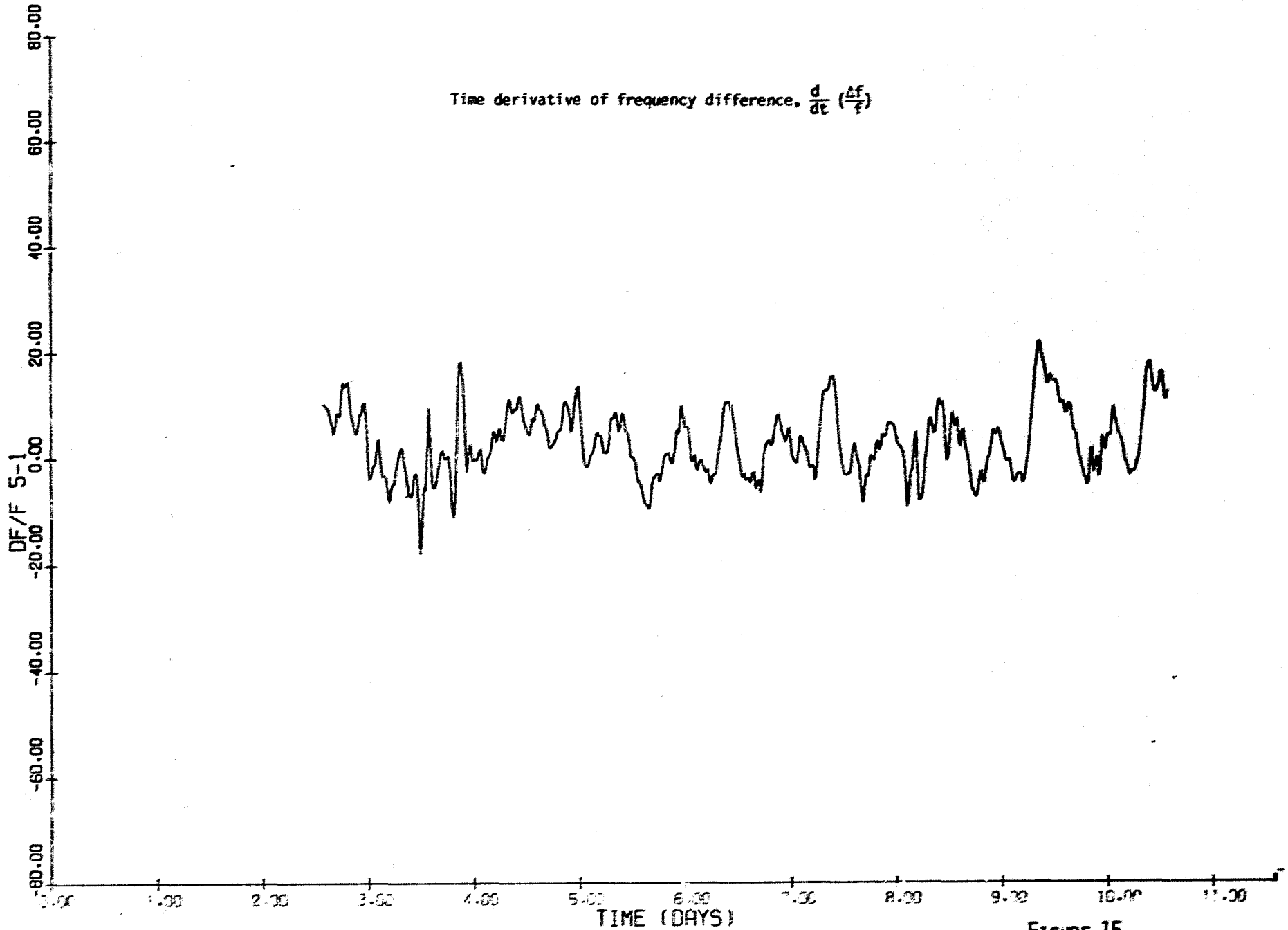

FIGURE 15

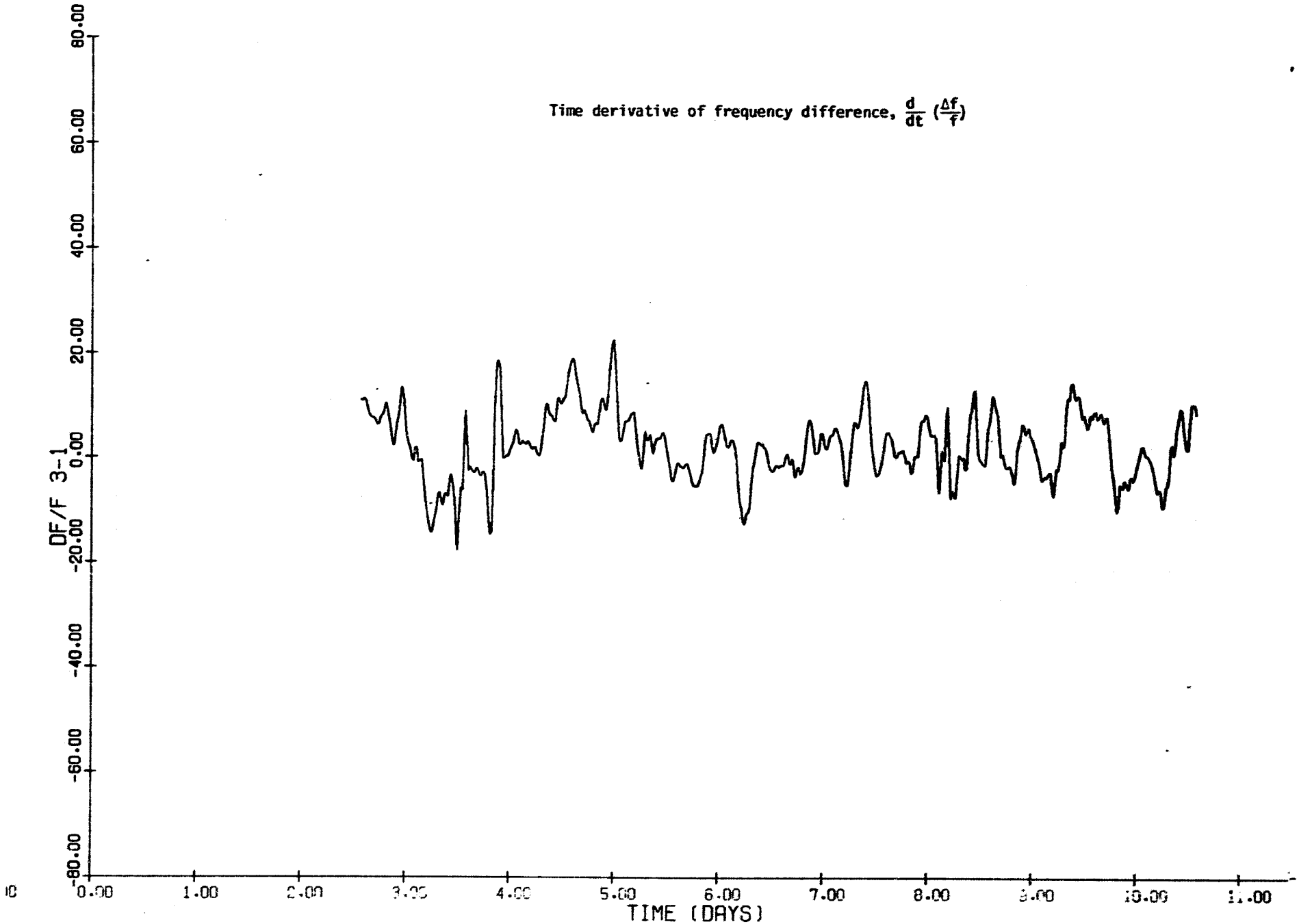
Time derivative of frequency difference, $\frac{d}{dt}(\frac{\Delta f}{f})$
DF/F 3-1
80.00
60.00
40.00
20.00
0.00
-20.00
-40.00
-60.00
-80.00
0.00
1.00
2.00
3.00
4.00
5.00
6.00
7.00
8.00
9.00
10.00
11.00
TIME (DAYS)

FIGURE 16

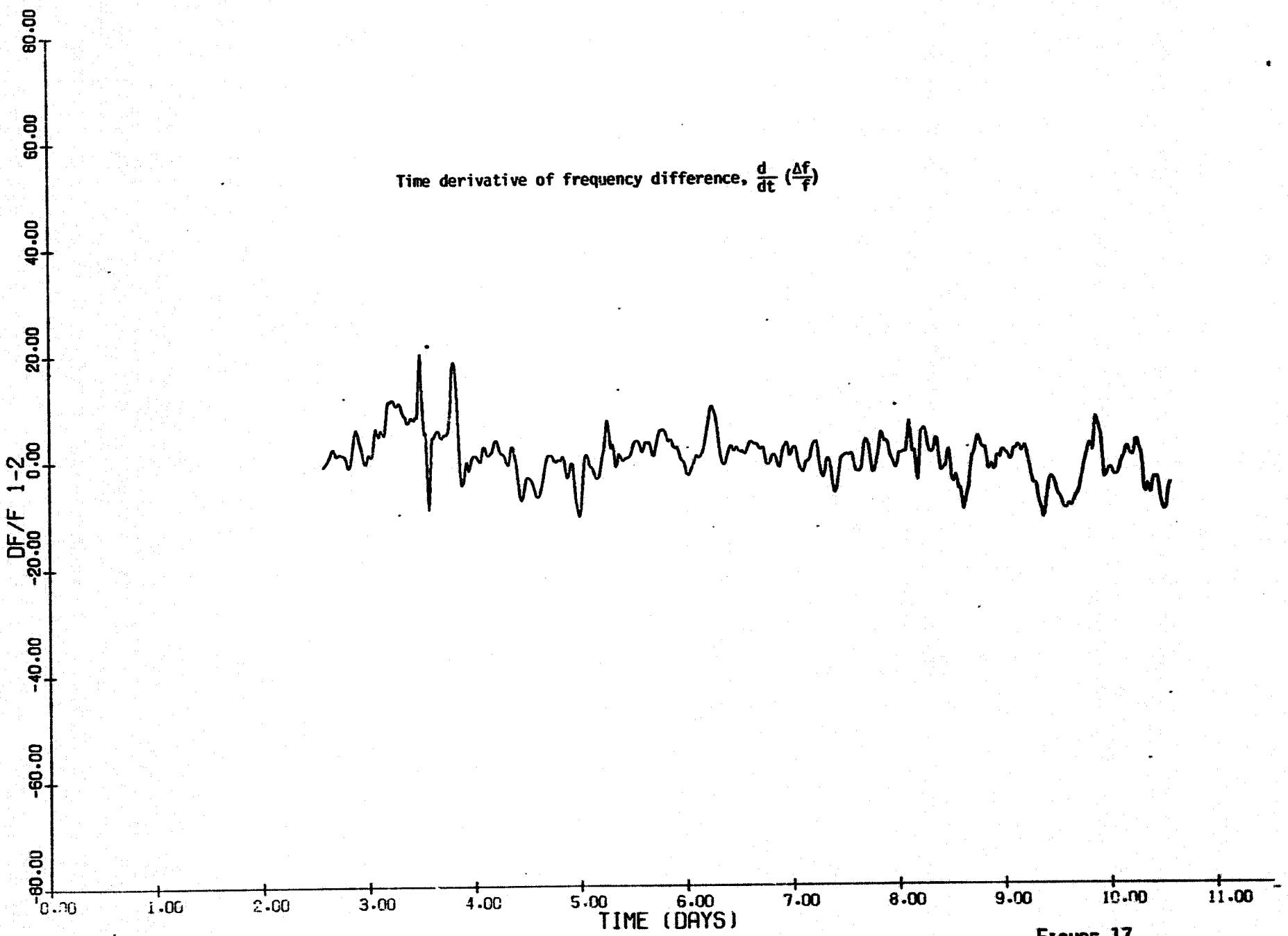
Time derivative of frequency difference, $\frac{d}{dt}(\frac{\Delta f}{f})$
DF/F 1-2
80.00
60.00
40.00
20.00
0.00
-20.00
-40.00
-60.00
-80.00
0.00
1.00
2.00
3.00
4.00
5.00
6.00
7.00
8.00
9.00
10.00
11.00
TIME (DAYS)

FIGURE 17

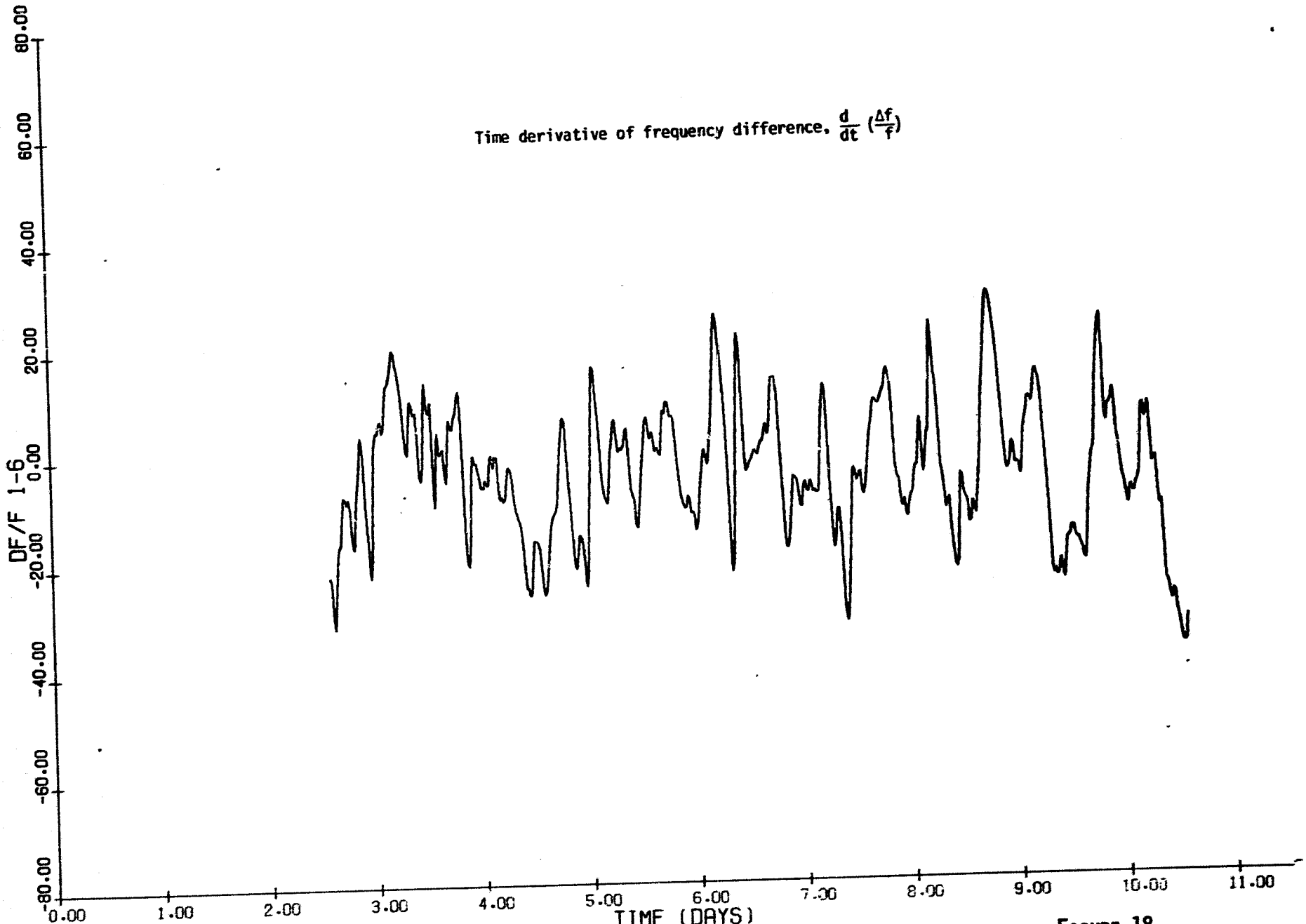
Time derivative of frequency difference, $\frac{d}{dt}(\frac{\Delta f}{f})$
DF/F 1-6
80.00
60.00
40.00
20.00
0.00
-20.00
-40.00
-60.00
-80.00
0.00
1.00
2.00
3.00
4.00
5.00
6.00
7.00
8.00
9.00
10.00
11.00
TIME (DAYS)

FIGURE 18

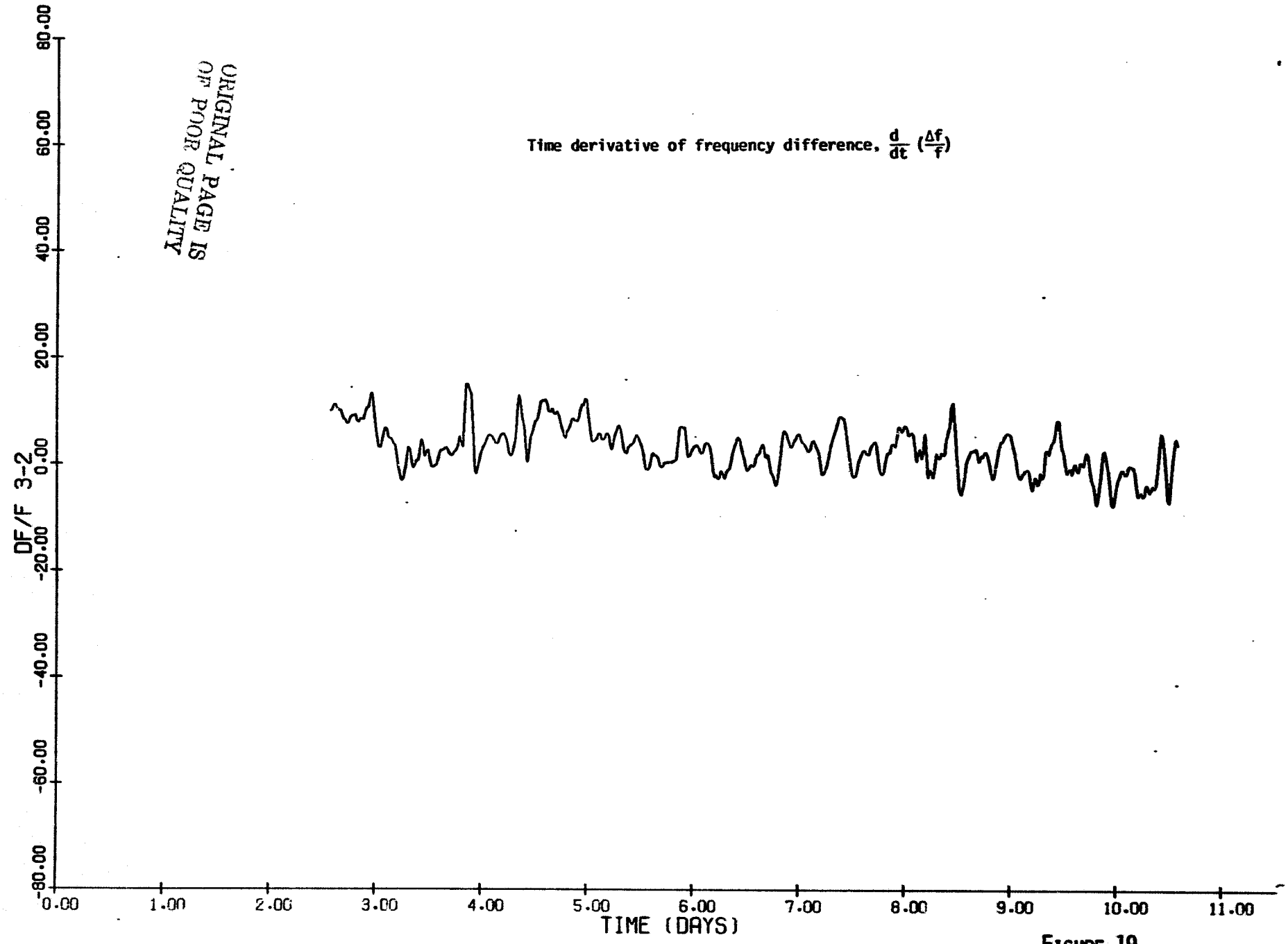

FIGURE 19

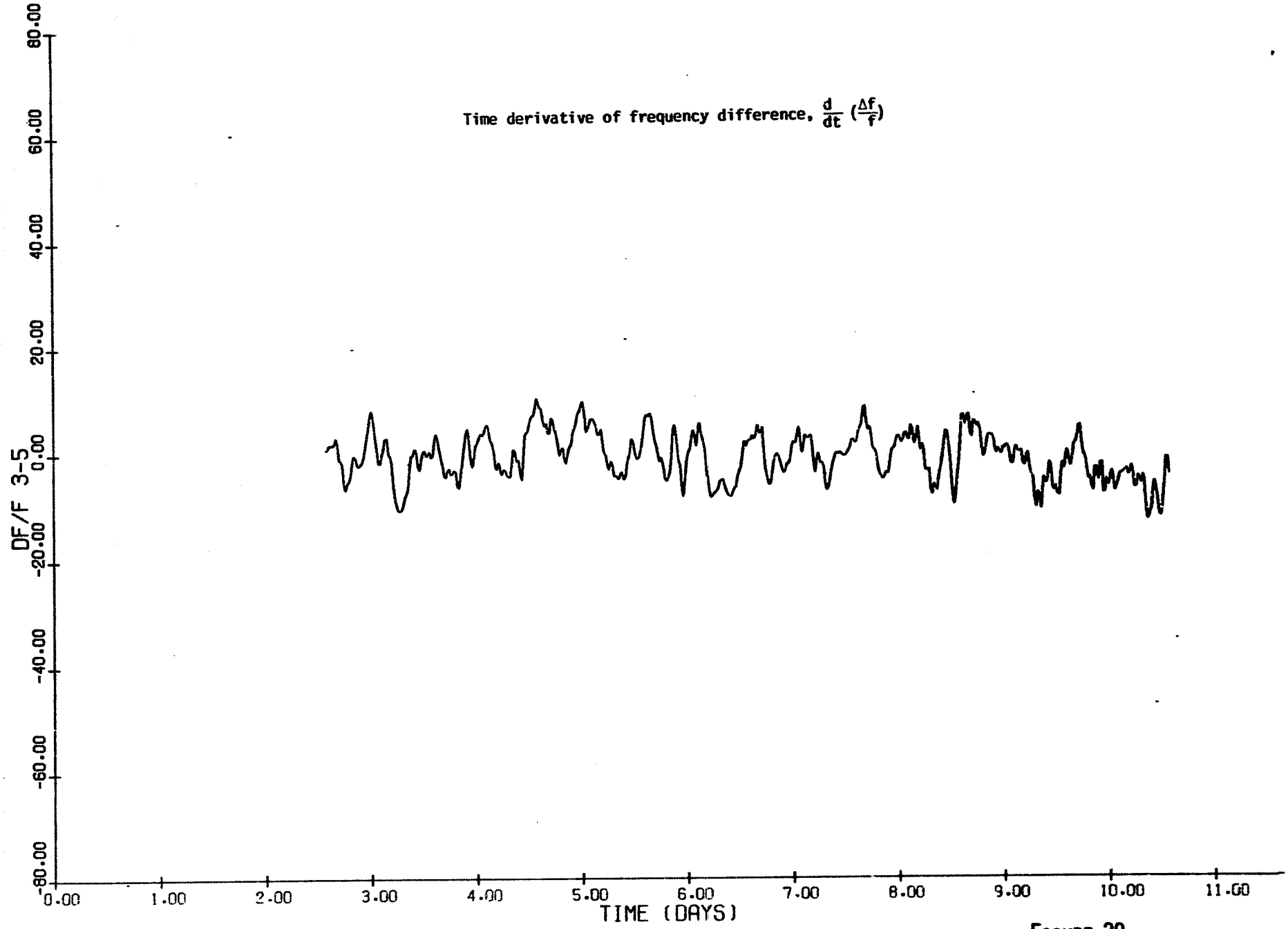
Time derivative of frequency difference, $\frac{d}{dt}\left(\frac{\Delta f}{f}\right)$
DF/F 3-5
80.00
60.00
40.00
20.00
0.00
-20.00
-40.00
-60.00
-80.00
0.00
1.00
2.00
3.00
4.00
5.00
6.00
7.00
8.00
9.00
10.00
11.00
TIME (DAYS)

FIGURE 20

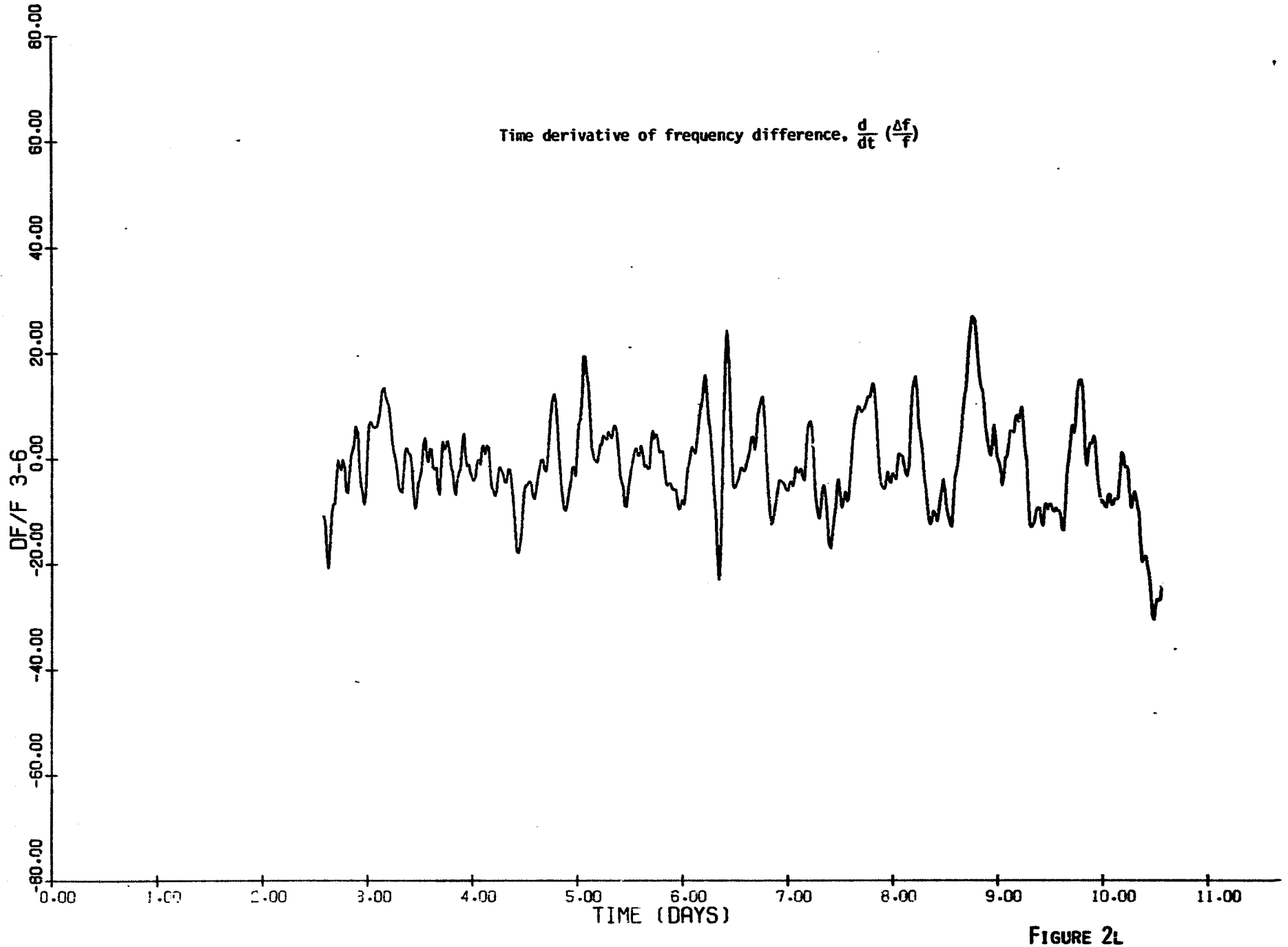
Time derivative of frequency difference, $\frac{d}{dt}\left(\frac{\Delta f}{f}\right)$
DF/F 3-6
80.00
60.00
40.00
20.00
0.00
-20.00
-40.00
-60.00
-80.00
0.00
1.00
2.00
3.00
4.00
5.00
6.00
7.00
8.00
9.00
10.00
11.00
TIME (DAYS)

FIGURE 2L

Time derivative of frequency difference, $\frac{d}{dt}\left(\frac{\Delta f}{f}\right)$

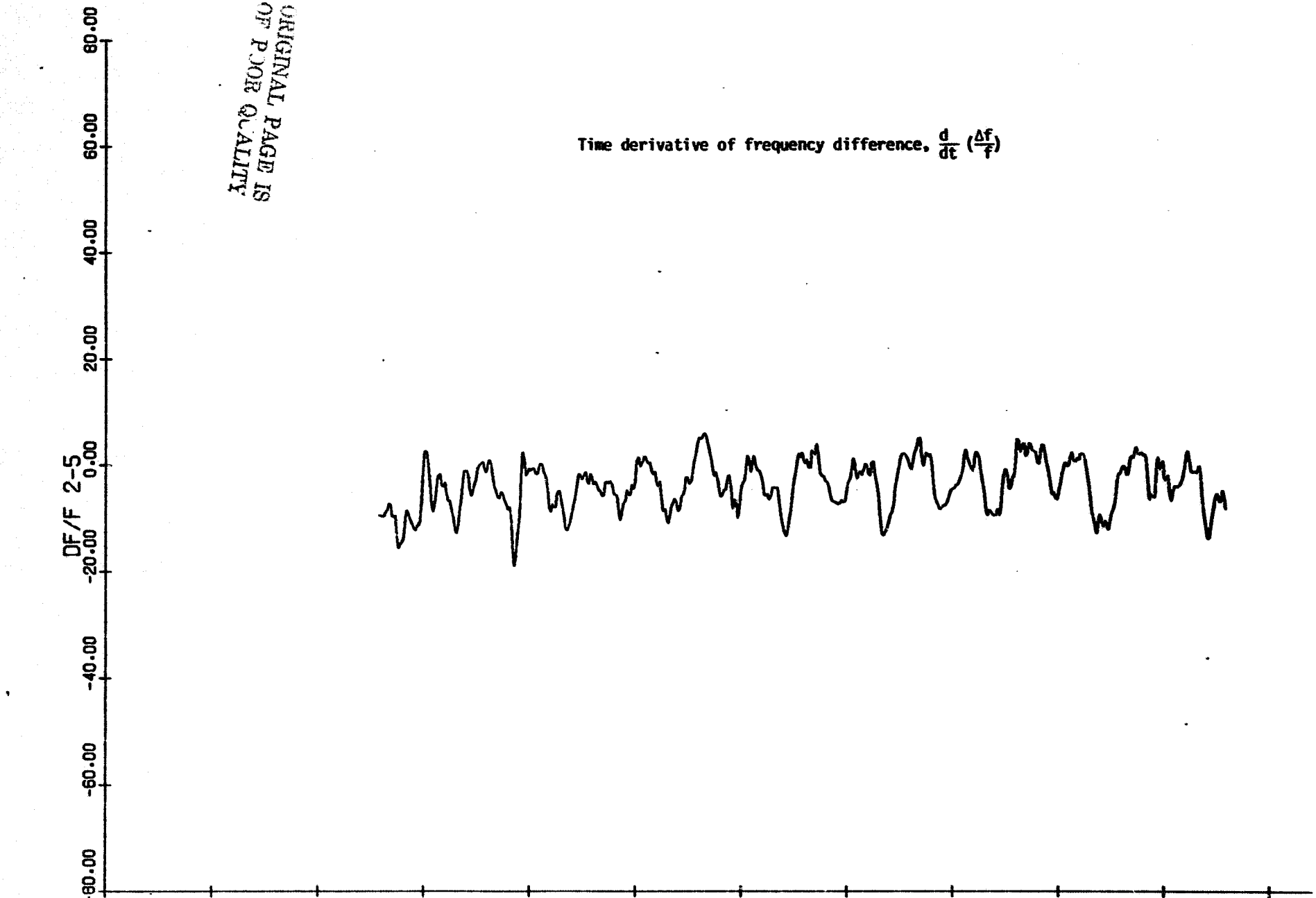

FIGURE 22

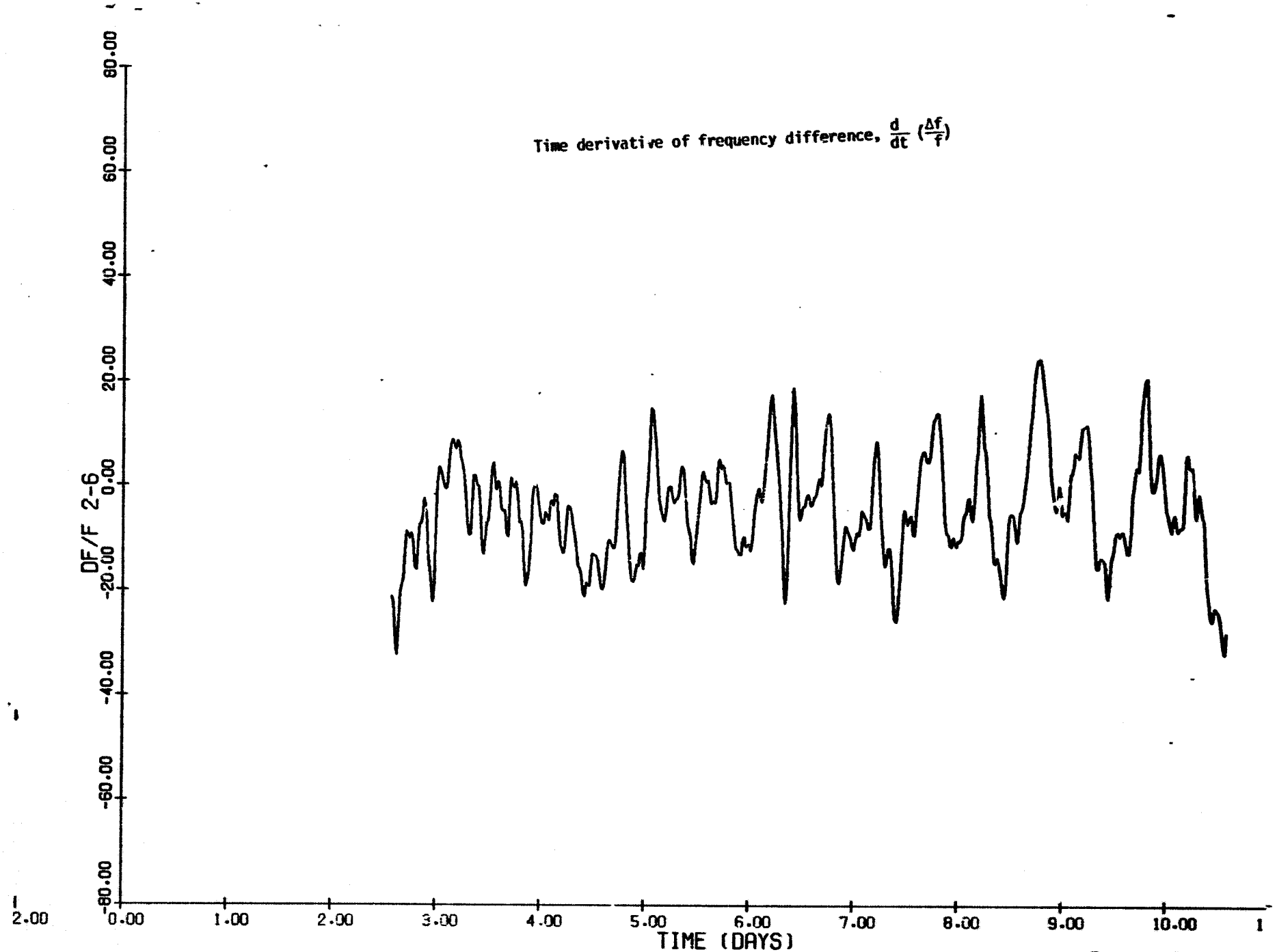
Time derivative of frequency difference, $\frac{d}{dt}\left(\frac{\Delta f}{f}\right)$
DF/F 2-6
80.00
60.00
40.00
20.00
0.00
-20.00
-40.00
-60.00
-80.00
2.00
0.00
1.00
2.00
3.00
4.00
5.00
6.00
7.00
8.00
9.00
10.00
1
TIME (DAYS)

FIGURE 23

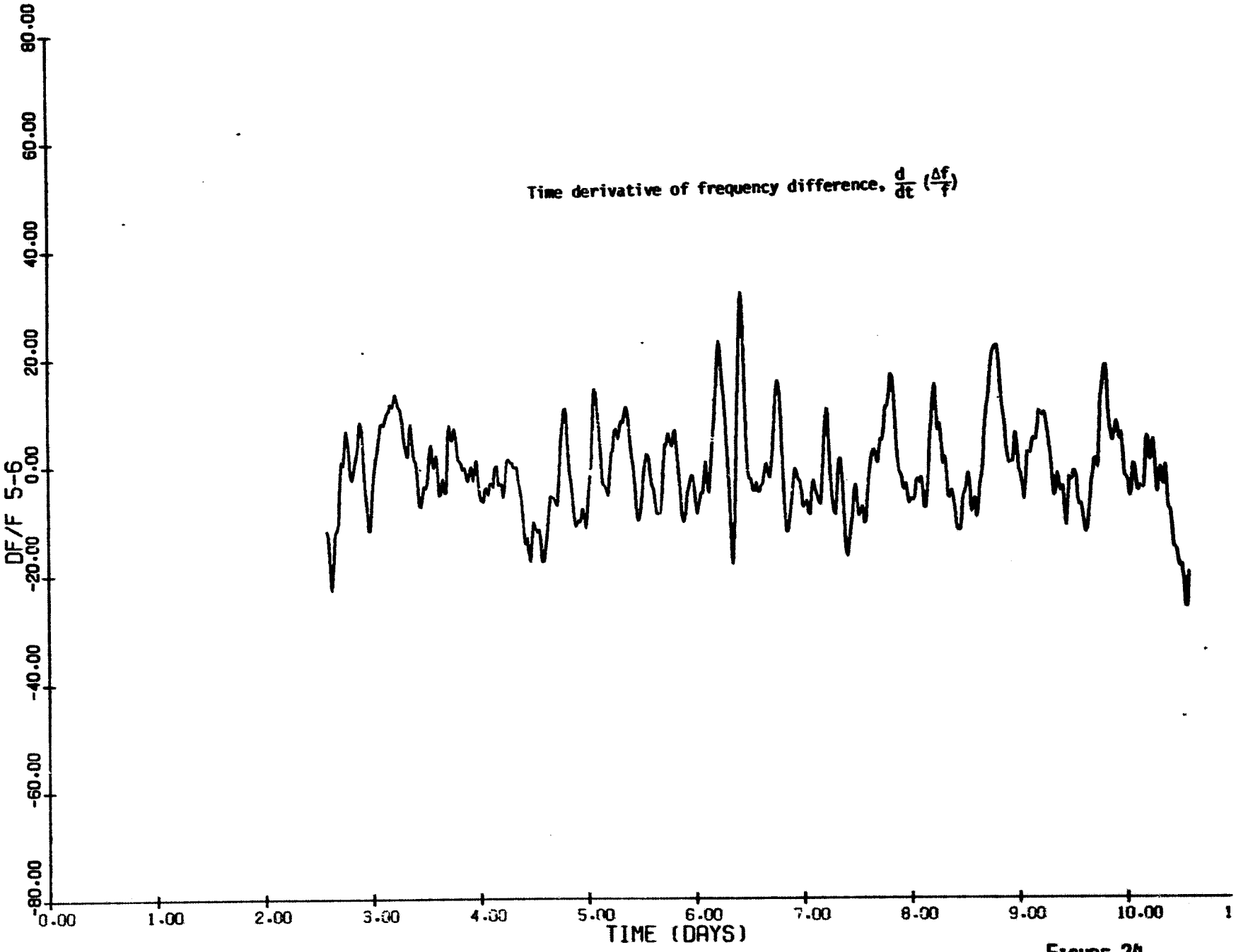
Time derivative of frequency difference, $\frac{d}{dt}(\frac{\Delta f}{f})$
DF/F 5-6
80.00
60.00
40.00
20.00
0.00
-20.00
-40.00
-60.00
-80.00
0.00
1.00
2.00
3.00
4.00
5.00
6.00
7.00
8.00
9.00
10.00
1
TIME (DAYS)

FIGURE 24

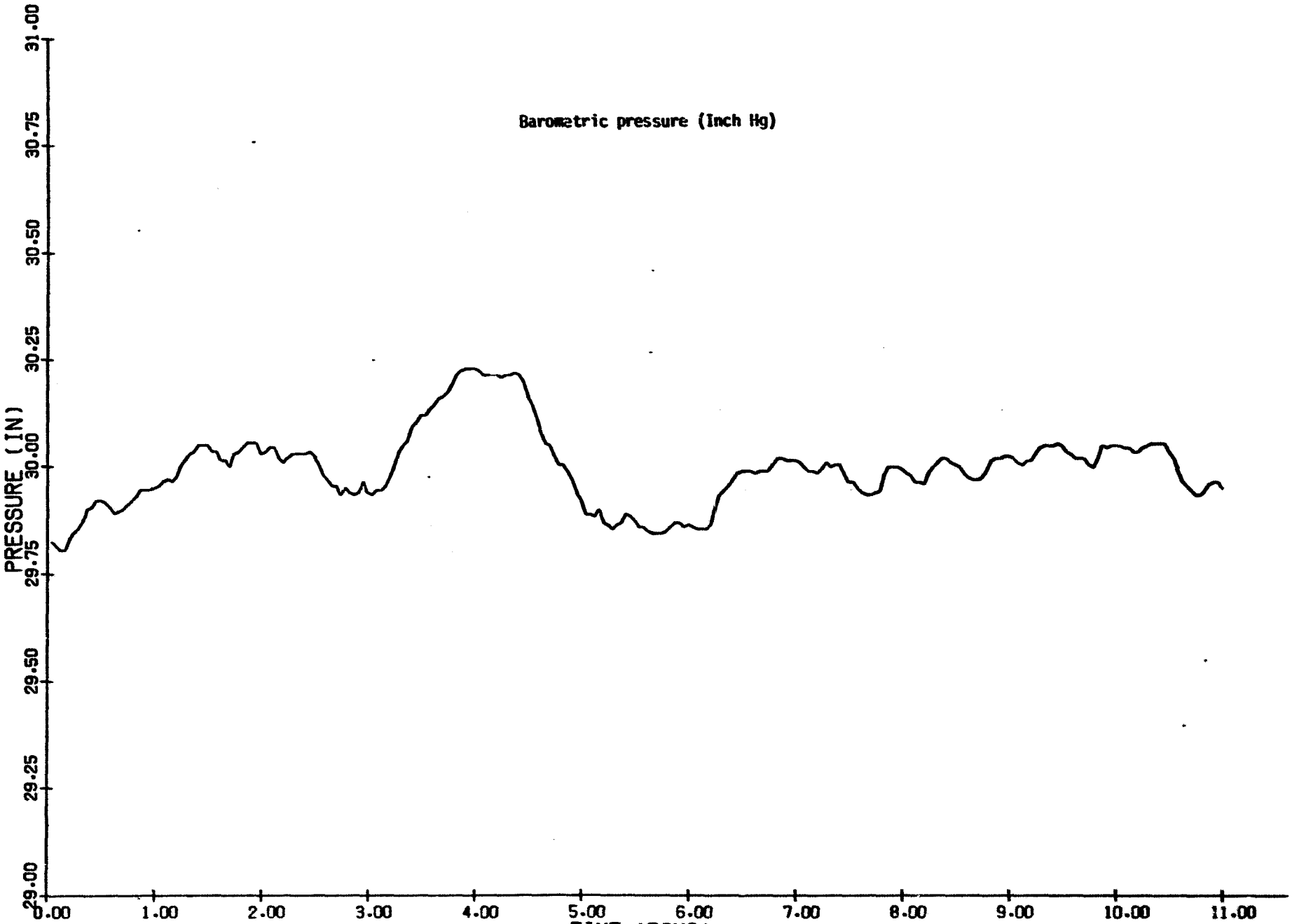
Barometric pressure (Inch Hg)
PRESSURE (IN)
31.00
30.75
30.50
30.25
30.00
29.75
29.50
29.25
29.00
0.00
1.00
2.00
3.00
4.00
5.00
6.00
7.00
8.00
9.00
10.00
11.00
TIME (DAYS)

FIGURE 25

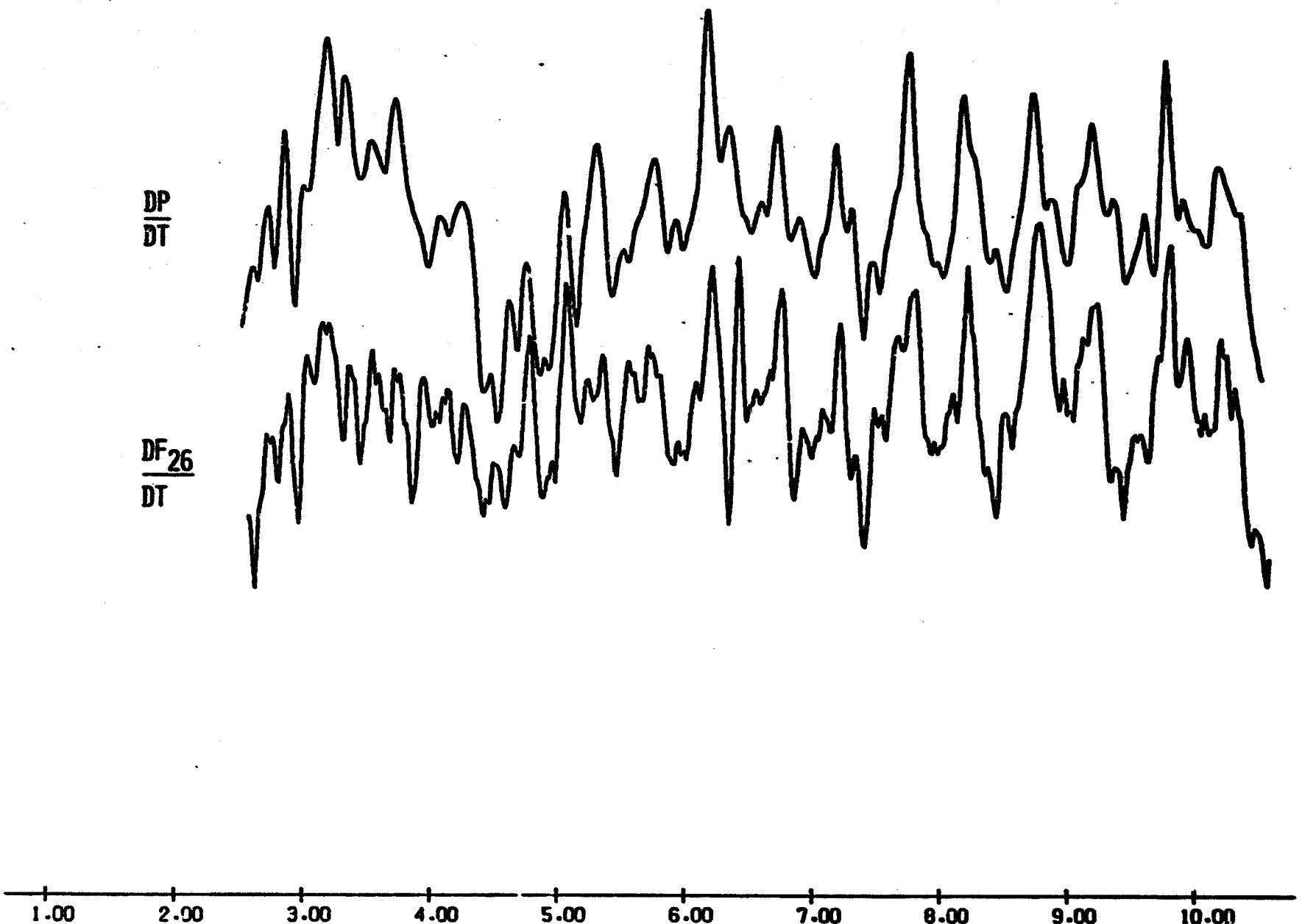

FIGURE 26